PB93-208544

U.S. Department
of Transportation
**Federal Railroad
Administration**

EVALUATION OF RAIL ROLLOVER DERAILMENT STUDY

Office of Research and
Development
Washington D.C. 20590

Stephen E. Mace

**Association of American Railroads
Transportation Test Center
Pueblo, Co 81001**

DOT/FRA/ORD-93/12

May 1993
Final Report

This document is available to the
U.S. public through the National
Technical Information Service
Springfield, Virginia 22161

REPRODUCED BY:
U.S. Department of Commerce
National Technical Information Service
Springfield, Virginia 22161
NTIS

METRIC CONVERSION FACTORS

Approximate Conversions to Metric Measures

Symbol	When You Know	Multiply by	To Find	Symbol
		LENGTH		
in	inches	*2.50	centimeters	cm
ft	feet	30.00	centimeters	cm
yd	yards	0.90	meters	m
mi	miles	1.60	kilometers	km
		AREA		
in^2	square inches	6.50	square centimeters	cm^2
ft^2	square feet	0.09	square meters	m^2
yd^2	square yards	0.80	square meters	m^2
mi^2	square miles	2.60	square kilometers	km^2
	acres	0.40	hectares	ha
		MASS (weight)		
oz	ounces	28.00	grams	g
lb	pounds	0.45	kilograms	kg
	short tons (2000 lb)	0.90	tonnes	t
		VOLUME		
tsp	teaspoons	5.00	milliliters	ml
Tbsp	tablespoons	15.00	milliliters	ml
fl oz	fluid ounces	30.00	milliliters	ml
c	cups	0.24	liters	l
pt	pints	0.47	liters	l
qt	quarts	0.95	liters	l
gal	gallons	3.80	liters	l
ft^3	cubic feet	0.03	cubic meters	m^3
yd^3	cubic yards	0.76	cubic meters	m^3
		TEMPERATURE (exact)		
°F	Fahrenheit temperature	5/9 (after subtracting 32)	Celsius temperature	°C

* 1 in. = 2.54 cm (exactly)

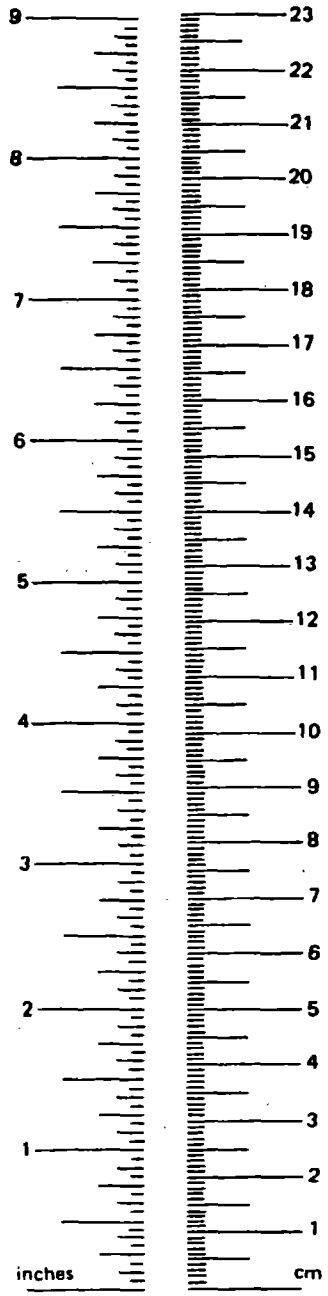

Approximate Conversions from Metric Measures

Symbol	When You Know	Multiply by	To Find	Symbol
		LENGTH		
mm	millimeters	0.04	inches	in
cm	centimeters	0.40	inches	in
m	meters	3.30	feet	ft
m	meters	1.10	yards	yd
km	kilometers	0.60	miles	mi
		AREA		
cm^2	square centim.	0.16	square inches	in^2
m^2	square meters	1.20	square yards	yd^2
km^2	square kilom.	0.40	square miles	mi^2
ha	hectares (10,000 m^2)	2.50	acres	
		MASS (weight)		
g	grams	0.035	ounces	oz
kg	kilograms	2.2	pounds	lb
t	tonnes (1000 kg)	1.1	short tons	
		VOLUME		
ml	milliliters	0.03	fluid ounces	fl oz
l	liters	2.10	pints	pt
l	liters	1.06	quarts	qt
l	liters	0.26	gallons	gal
m^3	cubic meters	36.00	cubic feet	ft^3
m^3	cubic meters	1.30	cubic yards	yd^3
		TEMPERATURE (exact)		
°C	Celsius temperature	9/5 (then add 32	Fahrenheit temperature	°F

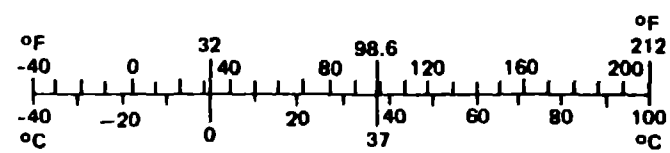

1. Report No.	2. PB93-208544	3. Recipient's Catalog No.
FRA/ORD-93/12		

4. Title and Subtitle	5. Report Date
Evaluation of Rail Rollover Derailment Study	May 1993
	6. Performing Organization Code
7. Author(s)	
Stephen E. Mace	8. Performing Organization Report No.
9. Performing Organization Name and Address	10. Work Unit No. (TRAIS)
Association of American Railroads Transportation Test Center P.O. Box 11130 Pueblo, CO 81001	11. Contract or Grant No. DTFR53-82-C-00282 Task Order 44
12. Sponsoring Agency Name and Address	13. Type of Report or Period Covered
U.S. Department of Transportation Federal Railroad Administration Office of Research and Development 400 Seventh Street SW Washington, D.C. 20590	November 1991 - June 1992
	14. Sponsoring Agency Code

15. Supplementary Notes

16. Abstract

Research conducted by the Association of American Railroads at the U.S. Department of Transportation, Transportation Test Center, Pueblo, Colorado, led to an understanding of the gage widening behavior exhibited by several 125-ton gondola cars and locomotives in a 6-degree curve of the Facility for Accelerated Service Testing (FAST), High Tonnage Loop (HTL). For the gondola cars, the cause of the gage widening was attributed to truck warp, a condition in which the side frames of a truck rotate relative to the bolster and both wheel sets develop large angles of attack. The truck frames were found to warp due to a combination of poor wheel/rail contact geometry, insufficient wheel tread taper, and rail lubrication applied to only the gage face of the high rail in the curve. The gage widening attributed to the locomotives was found to be a consequence of unbalanced traction forces applied to the high and low rails in the curve resulting from differential rail lubrication.

A unique two-phase approach was used to study the gage widening behavior, which consisted of actual track tests conducted on the HTL coupled with NUCARS simulations of the gondola cars.

The gage widening behavior was first observed in 1991 during operation of the FAST Heavy Axle Load (HAL) consist on the HTL. Concern over excessive gage widening prompted the Federal Railroad Administration to sponsor research aimed at understanding this behavior and assure the continued safe operation of the HAL train.

17. Key Words	18. Distribution Statement
Gage widening behavior 125-ton gondola cars & locomotives Angle of attack Truck Warp	This document is available through National Technical Information Service Springfield, VA 22161

19. Security Classification (of the report)	20. Security Classification (of this page)	21. No. of Pages	22. Price

Form DOT F 1700.7 (8-72)

EXECUTIVE SUMMARY

Research conducted by the Association of American Railroads (AAR), at the U.S. Department of Transportation, Transportation Test Center, Pueblo, Colorado, led to an understanding of the gage widening behavior exhibited by several 125-ton gondola cars and locomotives in a 6-degree curve of the Facility for Accelerated Service Testing (FAST), High Tonnage Loop (HTL). For the gondola cars, the cause of the gage widening was attributed to truck frame warp, a condition in which the side frames of a truck rotate relative to the bolster and both wheel sets develop large angles of attack. The truck frames were found to warp due to a combination of poor wheel/rail contact geometry, insufficient wheel tread taper, and rail lubrication applied to only the gage face of the high rail in the curve. The gage widening attributed to the locomotives was found to be a consequence of unbalanced traction forces applied to the high and low rails in the curve resulting from differential rail lubrication.

When the trucks of the gondola cars entered the curve entry spiral, the leading wheel set of each truck developed an angle of attack relative to the track and moved laterally into flange contact with the high rail. Due to high rail gage corner grinding, the flanging wheel contacted the rail at two points, one point of contact on the flange and the other on the tread. Each contact point developed longitudinal creep forces. The flange contact point, being at a much larger rolling radius than the low rail tread, produced a longitudinal force and steering moment that was in the proper direction to turn the truck in the curve. However, the high rail tread contact point was at a rolling radius that was no larger than that of the low rail tread and thus produced a longitudinal force and steering moment in the opposite direction to that of the flange. This steering moment acted to oppose the required truck rotation.

When both the head and gage face of the high rail were dry or uniformly lubricated, the longitudinal creep force developed by the wheel flange exceeded that of the tread, and a net steering moment was produced by the wheel set in the proper direction to turn the truck in the curve. However, when the gage face of the high rail was lubricated but the railhead remained dry, the wheel tread longitudinal creep force exceeded that of the flange and a net steering moment was produced by the wheel set that opposed the required truck rotation. As a result, large lateral forces were developed to turn the truck in the curve.

The large lateral forces developed to turn the truck in the curve also acted to warp the truck frame. When this occurred, both wheel sets of the truck developed large angles of attack, thereby, developing large gage widening forces. When several warped trucks were grouped together in the consist, gage widening exceeding 0.5 inch was produced.

A unique two-phase approach was used to study the gondola car gage widening behavior which consisted of actual track tests conducted on the HTL coupled with computer simulations of the gondola cars. The simulations were performed using NUCARS (New and Untried Car Analytic Regime Simulation), which is a rail vehicle dynamics model that predicts the response of any rail vehicle to any type of rail geometry. The simulations were essential to understanding this mechanism since they provided estimates of the wheel flange and tread contact forces that could not be measured in the track tests. The simulation and track test results that could be compared were found to be reasonably similar.

Locomotive gage widening behavior, which has been observed previously at FAST, was found to be a consequence of lubricating only one rail in the curve. In this situation, the locomotive developed much larger tractive (longitudinal) forces on one rail than the other. As a result, large truck turning moments were generated. When the high rail was lubricated and the low rail was dry, these turning moments were produced in a direction that caused both wheel sets in each truck to develop large angles of attack and spread the rails.

The gage widening behavior discussed above was observed in 1991 during operation of the FAST Heavy Axle Load (HAL) consist on the HTL. Concern over the excessive gage widening prompted the Federal Railroad Administration (FRA) to sponsor research aimed at understanding this behavior. The testing, conducted by the AAR, began in December 1991 and was completed in February 1992. The simulation studies and test data analysis continued throughout 1992. As a result of this research program, the following recommendations were made concerning operation of the HAL train.

1. Severe two point contact between the wheels of the HAL cars and the rails should be avoided by maintaining conformal or single-point contact wheel and rail profiles.

2. The combination of a dry low rail and a high rail with lubricated gage face and dry head in curves should be avoided by ensuring the high railhead is well lubricated and the low railhead is lightly lubricated.

3. In curves where gage corner grinding is practiced, the lateral track strength should be increased by installing elastic fasteners, rather than cut spikes.

4. Some means of increasing the warp restraint of three-piece trucks, such as frame bracing, should be used to reduce the incidences of truck frame warping and production of large gage widening forces.

The recommendations developed to address the HAL gage widening problem also apply to revenue service operations where, in curves, high rail gage corner grinding and flange lubrication are practiced.

Table of Contents

1.0 INTRODUCTION 1

2.0 OBJECTIVES 1

3.0 PROCEDURES 2
- 3.1 TECHNICAL APPROACH 2
  - 3.1.1 Gage Widening and Rail Rollover 2
  - 3.1.2 Truck Warp 3
  - 3.1.3 Truck Moments 5
  - 3.1.4 Truck Steering Moments 6
- 3.2 TRACK TEST PROCEDURES 9
  - 3.2.1 Baseline Car Test 9
  - 3.2.2 Bad Actor Car Test 10
  - 3.2.3 Truck Sequence and Tractive Effort Tests 10
- 3.3 MODELING PROCEDURES 11

4.0 MEASUREMENTS 11
- 4.1 ONBOARD MEASUREMENTS 12
  - 4.1.1 Baseline and Bad Actor Car Tests 12
  - 4.1.2 Truck Sequence Test 14
- 4.2 WAYSIDE MEASUREMENTS 14
- 4.3 WHEEL AND RAIL PROFILE MEASUREMENTS 15

5.0 RESULTS 15
- 5.1 BASELINE CAR ON DRY RAILS 16
  - 5.1.1 Onboard Measurements 16
  - 5.1.2 Wayside Measurements 18
- 5.2 BASELINE CAR ON LUBRICATED HIGH RAIL AND DRY LOW RAIL 18
  - 5.2.1 Onboard Measurements 18
  - 5.2.2 Wayside Measurements 20
- 5.3 BASELINE CAR ON LUBRICATED RAILS 20
  - 5.3.1 Onboard Measurements 20
  - 5.3.2 Wayside Measurements 22
- 5.4 BAD ACTOR CAR ON DRY RAILS 22
  - 5.4.1 Onboard Measurements 22

5.4.2 Wayside Measurements 23
5.5 BAD ACTOR CAR ON LUBRICATED HIGH RAIL AND DRY LOW RAIL 23
5.5.1 Onboard Measurements 23
5.5.2 Wayside Measurements 25
5.6 BAD ACTOR CAR ON LUBRICATED RAILS 25
5.6.1 Onboard Measurements 25
5.6.2 Wayside Measurements 26
5.7 TRUCK SEQUENCE TEST 26
5.8 WHEEL AND RAIL PROFILE MEASUREMENTS 30
5.9 MODEL WITH INSTRUMENTED WHEEL SET PROFILES 31
5.10 MODEL WITH CAR 406 WHEEL PROFILES 32
5.11 TRACTIVE EFFORT TEST 35
6.0 DISCUSSION OF RESULTS 37
7.0 CONCLUSIONS 38
8.0 RECOMMENDATIONS 40
References 41

List of Figures

Figure 1. Lateral and Vertical Wheel Forces Acting to Roll 2
Figure 2. Truck Frame Warped During Curve Negotiation 3
Figure 3. Moments Applied to a Three-Piece Truck 4
Figure 4. Truck Frame Steered During Curve Negotiation 5
Figure 5. Turning Moments Applied to Trucks 6
Figure 6. Required High Rail/Low Rail Diameter Difference 7
Figure 7. Wheel Set Rolling Diameter Variation 7
Figure 8. Wheel Set Longitudinal Creep Forces 8
Figure 9. Two-Point Contact Longitudinal Creep Forces 8
Figure 10. FAST-HTL Track 9
Figure 11. Baseline Car Test Consist 10
Figure 12. Bad Actor Car Test Consist 10
Figure 13. Truck Sequence Test Consist 11
Figure 14. Baseline Car Truck Moments on Dry Rails 17
Figure 15. Baseline Car Truck Angles on Dry Rails 18
Figure 16. Baseline Car Truck Moments on Lubricated High Rail and Dry Low Rail 19
Figure 17. Baseline Car Truck Angles on Lubricated High Rail and Dry Low Rail 20
Figure 18. Baseline Car Truck Moments on Lubricated Rails 21
Figure 19. Baseline Car Truck Angles on Lubricated Rails 21
Figure 20. Bad Actor Car Truck Moments on Dry Rails 22
Figure 21. Bad Actor Car Truck Angles on Dry Rails 23
Figure 22. Bad Actor Car Truck Moments on Lubricated High Rail and Dry Low Rail 24
Figure 23. Bad Actor Car Truck Angles on Lubricated High Rail and Dry Low Rail 24
Figure 24. Bad Actor Car Truck Moments on Lubricated Rails 25
Figure 25. Bad Actor Car Truck Angles on Lubricated Rails 26
Figure 26. Inside Rail Lateral Deflections and Forces with Lubricated Gage Face 27
Figure 27. Inside Rail Lateral Deflections and Forces with Lubricated Gage Face 28

Figure 28. Car 406 Truck Angles 30
Figure 29. Instrumented Wheel Set and Car 406 Wheel Profile 31
Figure 30. Instrumented Wheel Set Model Truck Moments on Lubricated Gage Face 31
Figure 31. Instrumented Wheel Set Model Truck Angles on Lubricated Gage Face 32
Figure 32. Car 406 Model Truck Moments on Lubricated Gage Face 33
Figure 33. Car 406 Model Truck Angles on Lubricated Gage Face 34
Figure 34. Inside Rail Lateral Deflections and Forces with Dry Rail 35
Figure 35. Inside Rail Lateral Deflections and Forces with Lubricated High Rail 36
Figure 36. Locomotive Truck Turning Moment 37

List of Tables

Table 1. Onboard Measurement List for Instrumented Wheel Set Tests 13
Table 2. Onboard Measurement List for Truck Sequence Tests 14
Table 3. Wayside Measurement List 15

1.0 INTRODUCTION

During operation of the Facility for Accelerated Service Testing (FAST), Heavy Axle Load (HAL) train in the spring and summer of 1991 at the Transportation Test Center, Pueblo, Colorado, several 125-ton cars were observed to produce low railhead lateral deflections in excess of 0.5 inch in Section 25 of the High Tonnage Loop (HTL). The largest deflections were measured in the Two-point Contact Grind Zone of the 6-degree curve in Section 25. It was also noted that most of the low rail gage side line spikes in the zone were pulled up 1 to 2 inches above the rail base. These observations indicated that the low rail in the area had been rolled outward by large gage widening forces produced by some of the HAL cars.

TTC engineers conducted an investigation to determine the causes of this unusual behavior. Several gage widening cars were removed from the HAL consist and inspected. No obvious defects were found. The cars were then assembled into a "mini-consist" and tested in Section 25 of the HTL. The effects of rail lubrication, train length, locomotive tractive effort, wheel profile, and rail profile on gage widening behavior were studied.

The FAST investigation did not provide a conclusive explanation of the gage widening behavior; however, several key areas were identified for further study. These were addressed by the Association of American Railroads (AAR) in a proposal to the Federal Railroad Administration (FRA) which solicited funds to continue investigating the HAL gage widening problem. In December 1991, the FRA responded by establishing a task order to conduct this investigation.

This report describes the test and modeling procedures used in the investigation, presents results from the testing and modeling activities, explains the gage widening behavior, and offers recommendations for correcting the gage widening problem.

2.0 OBJECTIVES

1. Confirm the essential safety of continued FAST operation.
2. Understand the origin of the excessive rail lateral deflection measured during recent FAST operations.
3. Establish guidelines, if necessary, for track strength and car mechanical conditions for both FAST and revenue operations.
4. Identify a strategy for continuing the FAST operation with "normal" track lubrication; i.e., with the high rail well lubricated and the low rail lightly lubricated.
5. Improve knowledge of the factors causing lateral rail deflections and potential gage widening derailments.

3.0 PROCEDURES

3.1 TECHNICAL APPROACH

3.1.1 Gage Widening and Rail Rollover

Gage widening occurs when large lateral forces are applied to both rails by the wheels of a passing rail vehicle. The forces act to roll the rails outward, and, if the amount of gage widening is sufficient, the wheel sets can drop between the rails.

The AAR uses a criterion called the *truck-side L/V ratio* as an indication of the potential for rail rollover. This criterion is simply the sum of the lateral forces of the wheels on one side of a truck divided by the sum of their vertical forces. In North America, the limit of an acceptable truck-side L/V ratio has been set at 0.6. Figure 1 illustrates how this value was derived. The positions of the wheels on the rails in the illustration represent the relative positions of the high and low rail wheels of a wheel set that is in flange contact with the high rail. For the high rail, a L/V ratio of 0.6 or larger will exceed the ratio d/h, and, if the rail has no torsional stiffness and is unrestrained by fasteners, it will roll over. For the low rail, however, the distance (d) at which the vertical load is applied is less than that of the high rail. This is because the high rail wheel contacts the rail with its flange, while the low rail wheel contacts the rail near the center of the railhead. As a result, the low rail d/h ratio will be smaller than that of the high rail ratio, dropping to approximately 0.4 for the situation where the low rail wheel contacts the center of the railhead.

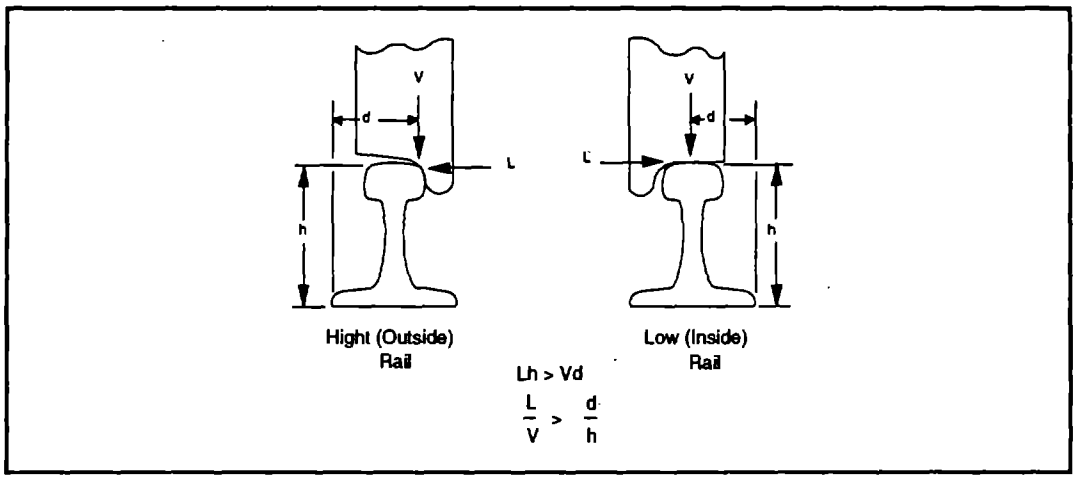

Figure 1. Lateral and Vertical Wheel Forces Acting to Roll the Rail Over

Much larger lateral deflections were measured on the low rail than on the high rail in the Section 25 curve during the earlier gage widening investigation sponsored by the FAST program. This result supports the idea that larger overturning moments were applied to the low rail than the high rail by a flanging wheel set because of the different lateral contact positions described above.

3.1.2 Truck Warp

Figure 2 shows a three-piece truck that has warped during spiral or curve negotiation. The truck frame has distorted in a manner that allows both wheel sets to develop large angles of attack. As a consequence of their large angles of attack, both wheel sets can produce large gage widening forces.

In order for the truck frame to distort, as shown in Figure 2, relative rotation must occur between the axle bearing adapters and the side frames, and between the side frames and the bolster. Relative rotation between these members can occur only if a moment is applied to the truck that exceeds its inherent warp restraint. The total warp restraint of a three-piece truck has a friction component and a stiffness component. Friction between the bearing adapters and side frames and in the snubbers produces the frictional component of the warp restraint. The stiffness component comes from the torsional stiffness of the bolster springs and from the snubbers.

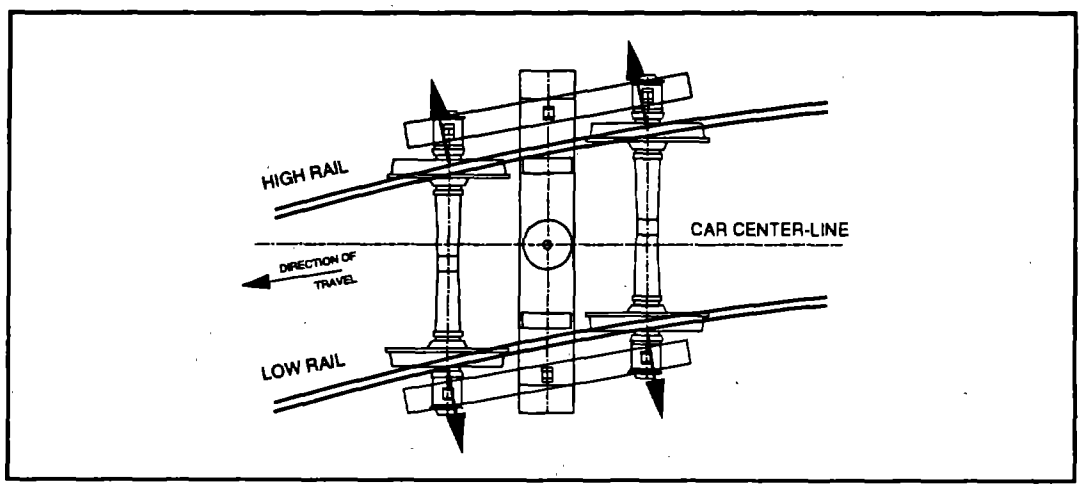

Figure 2. Truck Frame Warped During Curve Negotiation

The moment that acts to distort the truck frame is called the warp moment and is produced by lateral forces at the wheel and rails, as shown in Figure 3. It is produced in reaction to two other truck moments - the turning and steering moments. The turning moment is created by friction in the center bowl and side bearing connections between the truck and car body. The steering moment is produced by longitudinal creep forces developed between the wheels and rails. Figure 3 shows moment directions that are typical for the leading truck in a car negotiating the entry spiral of a curve.

Because the three truck moments must balance, the warp moment may be thought of as the sum of the turning and steering moments. The turning and steering moments can be applied to the truck in either direction, thus the resulting warp moment may be produced in either direction. Figure 2 shows a truck that has been distorted by a positive warp moment. The resulting distortion is in the proper direction to allow both wheel sets to develop large angles of attack. This will be referred to as the *warp* direction. Figure 4 shows a three-piece truck that has been distorted by a negative warp moment. In contrast to the positive warp moment case, the truck frame distorts in the opposite direction. The leading wheel set is in flange contact with the high rail and has developed a large angle of attack. The trailing wheel set, however, remains radially aligned with the curve. This direction of distortion will be referred to as *steer*. It is important to distinguish between the two directions of truck distortion. Warp distortion, where both wheel sets develop large angles of attack, can lead to the production of large gage widening forces. Steer distortion, however, does not.

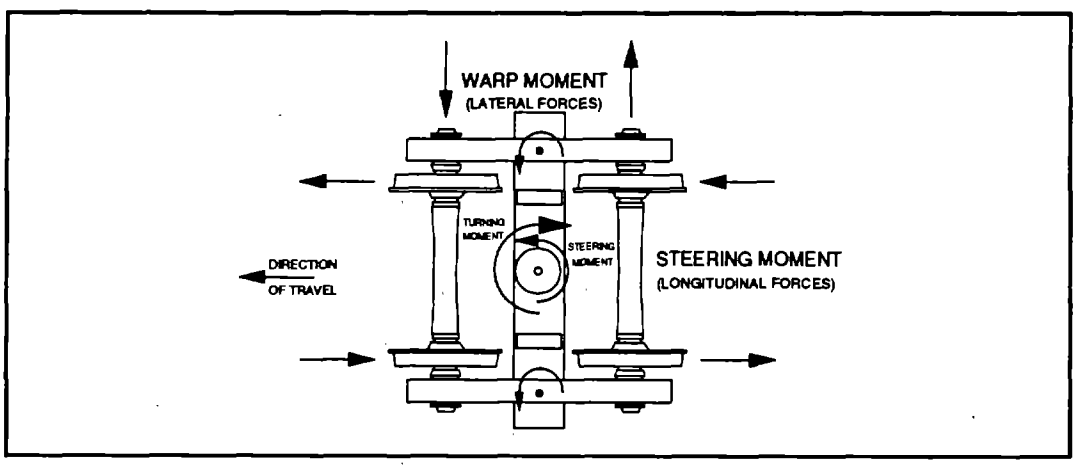

Figure 3. Moments Applied to a Three-Piece Truck

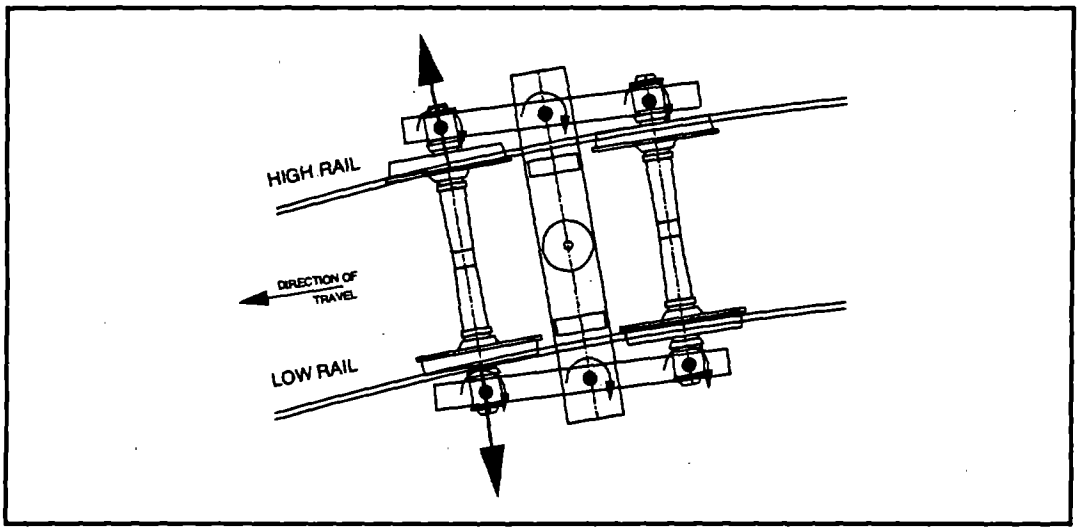

Figure 4. Truck Frame Steered During Curve Negotiation

3.1.3 Truck Moments

As discussed in the previous section, truck distortion may occur in either the warp or steer direction, depending on the direction and magnitude of the warp moment. Gage widening behavior, however, is associated only with truck distortion in the warp direction.

Truck warp distortion is produced by a positive warp moment; i.e. a warp moment that acts in the direction to turn the truck in the curve. A positive warp moment reaction will be produced when the net of the truck turning and steering moments opposes the required rotation of the truck in the curve. This requires that both the turning and steering moments be in the direction to oppose truck rotation or that the moment opposing rotation exceeds that assisting rotation.

For a leading truck, this situation is not uncommon. The turning moment applied to the leading truck by the car body in a spiral always opposes rotation, as shown in Figure 5. If the net steering moment generated by the wheel sets in the truck is also in this direction, or is lower in magnitude than the turning moment, then a warp moment reaction will be produced in the direction to warp the truck.

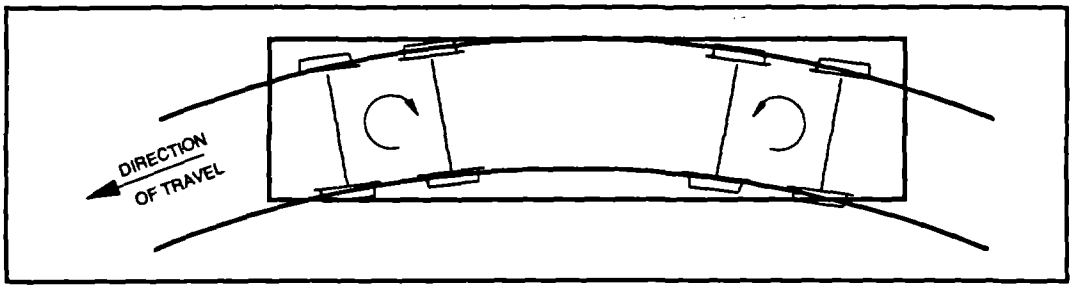

Figure 5. Turning Moments Applied to Trucks

This situation is different for the trailing truck. As shown in Figure 5, the turning moment applied to the trailing truck by the car body always assists rotation. The only way to generate a warp moment reaction in the direction to warp the truck is to produce a very large steering moment that opposes rotation of the truck. In order to warp the truck, the magnitude of this "anti-steering" moment must be larger than the turning moment by an amount exceeding the warp restraint of the truck.

The bad actor cars that produced excessive gage widening did so with both leading and trailing trucks. Thus, the trailing trucks must have been producing large "anti-steering" moments in the test curve. The origin of these "anti-steering" moments is the focus of this investigation. The next section describes how these "anti-steering" moments might be produced.

3.1.4 Truck Steering Moments

In the curve shown in Figure 6, the high rail wheel of the wheel set must negotiate a longer rail than the low rail wheel, but because the wheels are connected by a rigid axle, the two wheels must rotate at the same speed. In order to avoid slippage of one of the wheels on the rail, the rolling radius of the high rail wheel should be larger than that of the low rail wheel by the proper amount for the curve. Thus, rail wheels are given a profile such that they have a range of rolling diameters as they shift laterally on the rails, as shown in Figure 7.

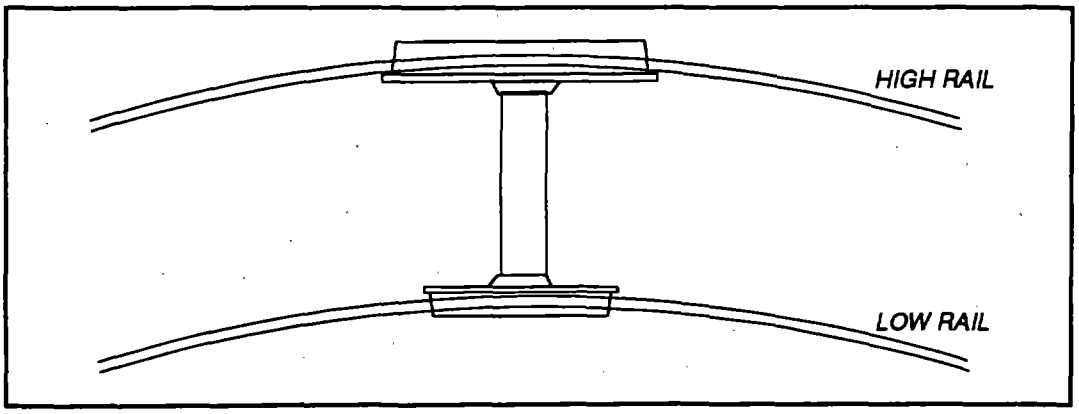

Figure 6. Required High Rail/Low Rail Diameter Difference

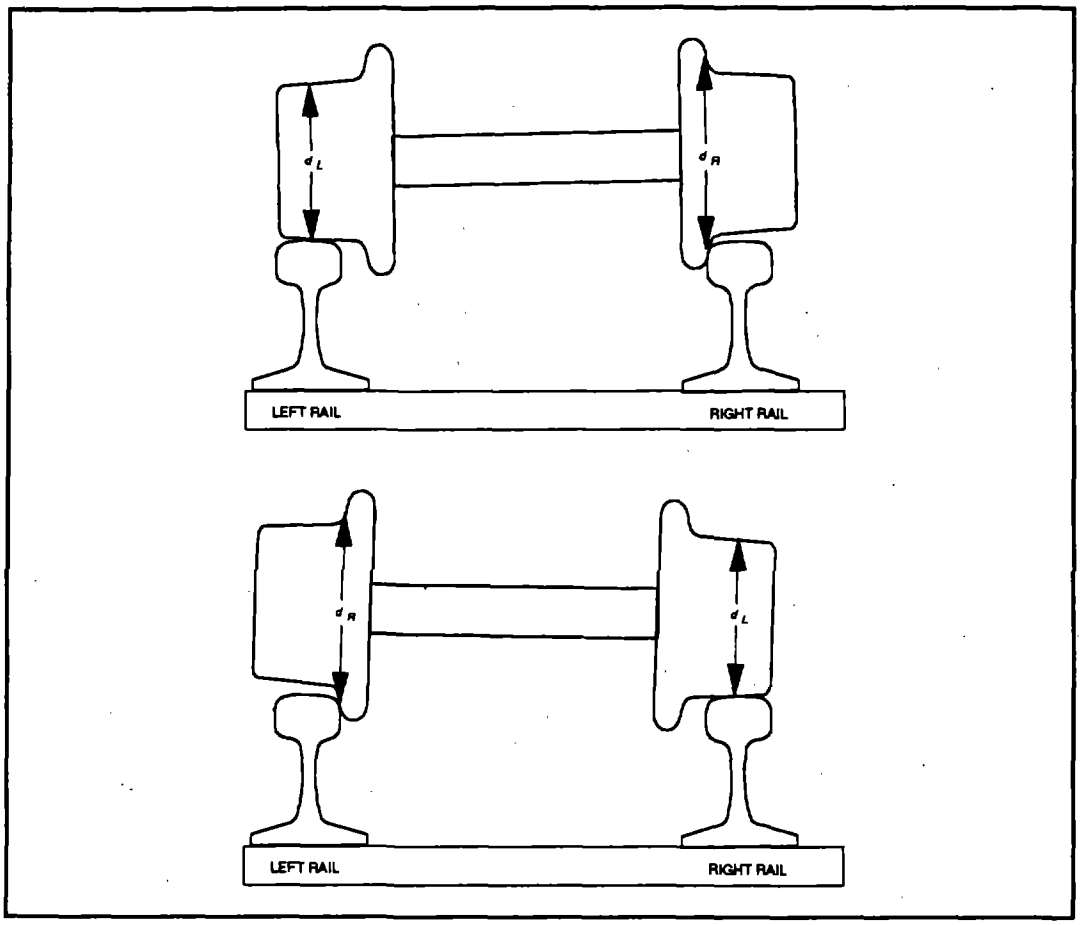

Figure 7. Wheel Set Rolling Diameter Variation

Figure 8 shows the longitudinal creep forces that are generated by a wheel set as it shifts laterally on the rail. As the high rail wheel moves from tread to flange contact with the rail, the direction of the longitudinal creep forces change as shown. The net steering moment produced by these forces also changes direction. Now consider the situation shown in Figure 9 where the high rail wheel contacts the rail at *two distinct points,* one point on the flange and the other out on the tread.[1] The flange contact point produces a forward or positive longitudinal force, and the tread produces a longitudinal force in the opposite direction. The net longitudinal force produced by the wheel is the difference between these forces. Depending on the relative magnitude of the flange and tread longitudinal creep forces, the steering moment may be positive, negative, or zero. If the tread longitudinal force exceeds that of the flange, then an "anti-steering" moment, or moment that opposes rotation of the wheel set, will be produced.

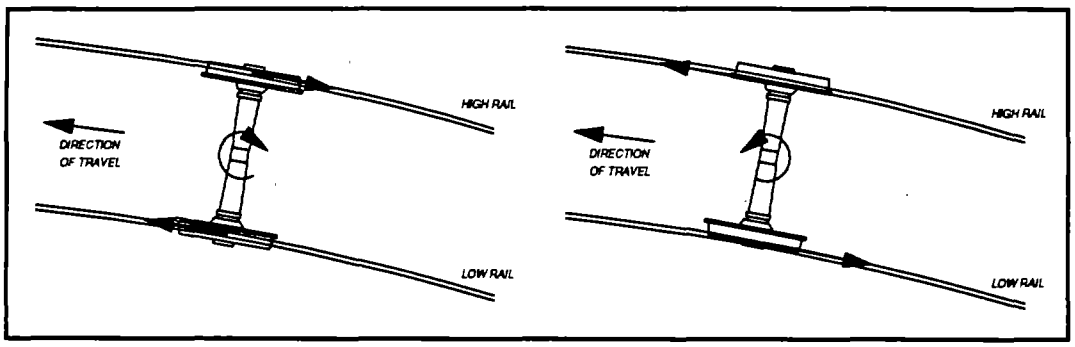

Figure 8. Wheel Set Longitudinal Creep Forces

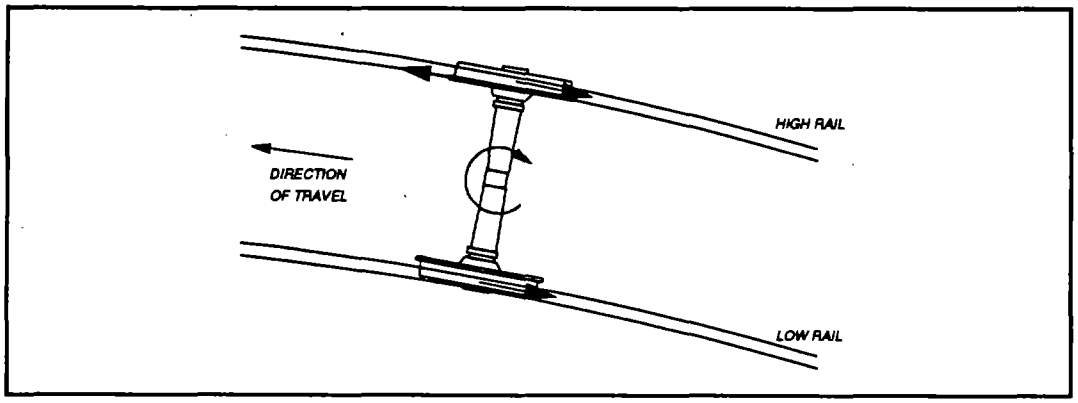

Figure 9. Two-Point Contact Longitudinal Creep Forces

3.2 TRACK TEST PROCEDURES

Four track tests, referred to as the Baseline Car, Bad Actor Car, Truck Sequence and Tractive Effort Tests, were conducted on the FAST-HTL. The Baseline Car and Bad Actor Car Tests were designed to compare the truck moments, truck-side L/V ratios, and truck frame warp characteristics of a gage widening car (the bad actor car), and a normal or baseline car. The Truck Sequence and Tractive Effort Tests were originally designed to study the effects of adjacent gage widening trucks and locomotive tractive effort on the maximum gage widening.

Figure 10 is a diagram of the FAST-HTL. Testing activities were concentrated in the 6-degree left hand curve of Section 25, where the greatest gage widening was previously measured. This curve contains rails with various profiles in support of ongoing HAL experiments.

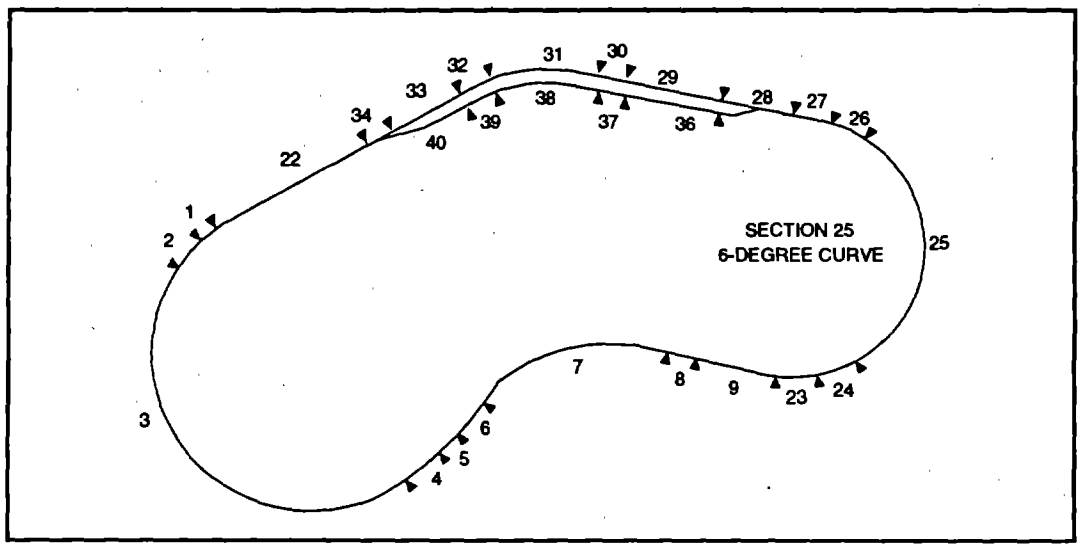

Figure 10. FAST-HTL Track

3.2.1 Baseline Car Test

FAST car 310 was selected from the HAL consist for the Baseline Car Test since it had no history of excessive gage widening. Instrumented wheel sets were installed in the trailing truck of the car. The car was then coupled to the AAR 207 Instrumentation Car and placed in the test consist, as shown in Figure 11. The test consist operated at 40 mph in the counterclockwise (CCW) direction on the HTL without lubrication applied to the rails. Measurements were recorded from both the onboard and wayside instrumentation sys-

tems. Top of rail and gage face friction were periodically measured with a tribometer. Next, lubrication was applied to the high rail in Section 25 and the tests repeated. Finally, both rails in Section 25 were lubricated and the tests repeated.

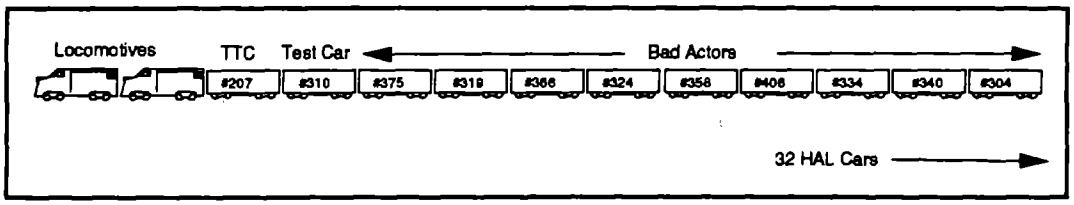

Figure 11. Baseline Car Test Consist

3.2.2 Bad Actor Car Test

FAST car 406 was selected from the HAL consist for the Bad Actor Car Test because it had previously produced excessive gage widening. Instrumented wheel sets were installed in the trailing truck of the car. The car was then coupled to the AAR 207 Instrumentation Car and placed in the test consist, as shown in Figure 12. The test consist operated at 40 mph in the CCW direction on the HTL without lubrication applied to the rails. Measurements were recorded from both the onboard and wayside instrumentation systems. Top of rail and gage face friction were periodically measured with a tribometer. Next, lubrication was applied to the high rail in Section 25 and the tests repeated. Finally, both rails in Section 25 were lubricated and the tests repeated.

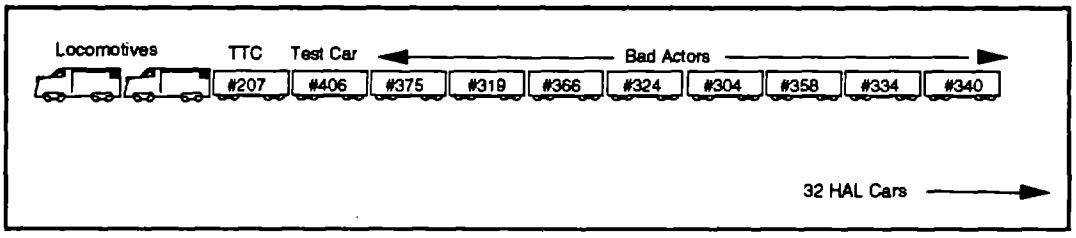

Figure 12. Bad Actor Car Test Consist

3.2.3 Truck Sequence and Tractive Effort Tests

The Truck Sequence Test procedure was modified to measure the performance of the test cars equipped with wheel sets from bad actor trucks to test the idea that the gage widening behavior was a consequence of poor wheel/rail contact geometry.

The Truck Sequence and Tractive Effort Tests were conducted together with the consist depicted in Figure 13. Several wheel set changes were incorporated in the Truck Sequence Test to demonstrate the effect of wheel/rail contact geometry on gage widening. The instrumented wheel sets used in the trailing truck of FAST car 406 during the Bad Actor Car Test were exchanged for the car's original wheel sets. Also, the original wheel sets of FAST car 307, a normal car, and FAST car 366, a bad actor car, were exchanged to study the effect of wheel profiles on gage widening behavior.

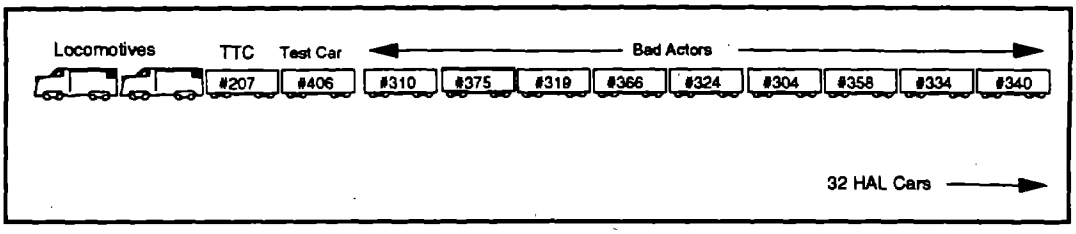

Figure 13. Truck Sequence Test Consist

The consist operated in the CCW direction through Section 25 of the HAL with no rail lubrication, with high rail lubrication, and with both rails lubricated. Test were conducted at 20 and 40 mph. Truck rotation angles and truck frame geometry were recorded for FAST car 406. Data were also recorded for the entire consist from the two wayside instrumentation sites in Section 25.

3.3 MODELING PROCEDURES

Two models of the HAL cars were developed for the simulation. The first model used wheel profiles measured from the instrumented wheel sets. And the second model used wheel profiles measured from the trailing truck of the HAL car 406, a bad actor car. Both models used the rail profiles measured at the Two-point Contact Grind Zone wayside measurement site. The models were run on track with a 6-degree left-hand curve and 5 inches of superelevation, duplicating the HAL Section 25 curve. Track lubrication conditions were varied from both rails dry to both railheads dry and the high rail gage face lubricated. The models were operated at 39 mph to match the test consist operating speed.

4.0 MEASUREMENTS

The following measurements were taken during the track test and were also available from the simulations.

4.1 ONBOARD MEASUREMENTS

4.1.1 Baseline and Bad Actor Car Tests

Instrumented wheel sets were installed in the trailing trucks of the baseline and bad actor cars to measure vertical, lateral, and longitudinal wheel forces. Displacement transducers were installed in each test truck to measure bolster rotation displacements, truck frame warp displacements, and wheel set to side frame longitudinal displacements. These direct measurements were used to produce several synthetic data channels using the equations listed below. Table 1 lists all of the direct and synthetic measurements.

$$M_{(s)} = (LO_{(l)} + LO_{(t)})*60.0$$

$$M_{(w)} = (L_{(ll)} + L_{(lr)}) - (L_{(tl)} + L_{(tr)})$$

$$M_{(t)} = M_{(s)} + M_{(w)}$$

$$TSLV_{(l)} = (L_{(ll)} + L_{(tl)})/(V_{(ll)} + V_{(tl)})$$

$$TSLV_{(r)} = (L_{(lr)} + L_{(tr)})/(V_{(lr)} + V_{(tr)})$$

$$A_{(w)} = (D_{(ll)} - D_{(tl)} + D_{(lr)} - D_{(tr)})/144$$

where:

$M_{(s)}$ - steering moment

$M_{(w)}$ - warp moment

$M_{(t)}$ - turning moment

$LO_{(l)}, LO_{(t)}$ - leading/trailing wheel longitudinal force (kips)

$L_{(ll)}, L_{(lr)}, L_{(tl)}, l_{(tr)}$ - leading/trailing/left/right wheel lateral force (kips)

$V_{(ll)}, V_{(lr)}, V_{(tl)}, V_{(tr)}$ - leading/trailing/left/right wheel vertical force (kips)

$TSLV_{(1)}$ - left truck-side L/V ratio

$TSLV_{(r)}$ - right truck-side L/V ratio

$A_{(w)}$ - Average truck frame warp angle (mradians)

$D_{(ll)}, D_{(lr)}, D_{(tl)}, D_{(tr)}$ - leading/trailing/left/right bols./s.f. lateral displ.(in.)

Table 1. Onboard Measurement List for Instrumented Wheel Set Tests

Measurement No.	Name	Units	Location
1	Lead Left Vertical Force	kips	Test Truck
2	Lead Left Lateral Force	kips	Test Truck
3	Lead Left L/V Ratio	kips	Test Truck
4	Lead Right Vertical Force	kips	Test Truck
5	Lead Right Lateral Force	kips	Test Truck
6	Lead Right L/V Ratio	kips	Test Truck
7	Trail Left Vertical Force	kips	Test Truck
8	Trail Left Lateral Force	kips	Test Truck
9	Trail Left L/V Ratio	kips	Test Truck
10	Trail Right Vertical Force	kips	Test Truck
11	Trail Right Lateral Force	kips	Test Truck
12	Trail Right L/V Ratio	kips	Test Truck
13	Lead Wheel Set Long. Force	kips	Test Truck
14	Trail Wheel Set Long. Force	kips	Test Truck
15	Lead Left BA/Side Frame Lat.	inch	Test Truck
16	Lead Right BA/Side Frame Lat.	inch	Test Truck
17	Trail Left BA/Side Frame Lat.	inch	Test Truck
18	Trail Right BA/Side Frame Lat.	inch	Test Truck
19	Lead Left BA/Side Frame Long.	inch	Test Truck
20	Lead Right BA/Side Frame Long.	inch	Test Truck
21	Trail Left BA/Side Frame Long.	inch	Test Truck
22	Trail Right BA/Side Frame Long.	inch	Test Truck
23	Bolster/Body Vertical Displ.	inch	Test Truck
24	Train Speed	mph	Instr. Car
25	Automatic Location Device	volts	Test Truck
26	Left Truck-Side L/V Ratio	L/V	Synthetic
27	Right Truck-Side L/V Ratio	L/V	Synthetic
28	Truck Steering Moment	kip-inch	Synthetic
29	Truck Warp Moment	kip-inch	Synthetic
30	Truck Turning Moment	kip-inch	Synthetic
31	Average Side Frame/Bolster Warp	mradians	Synthetic

4.1.2 Truck Sequence Test

The instrumented wheel sets were removed from the trailing truck of car 406 for the Truck Sequence Test. Table 2 lists the displacement measurements that were taken during the test.

Table 2. Onboard Measurement List for Truck Sequence Tests

Measurement No.	Name	Units	Location
1	Lead Left BA/Side Frame Lat.	inch	Test Truck
2	Lead Right BA/Side Frame Lat.	inch	Test Truck
3	Trail Left BA/Side Frame Lat.	inch	Test Truck
4	Trail Right BA/Side Frame Lat.	inch	Test Truck
5	Lead Left BA/Side Frame Long.	inch	Test Truck
6	Lead Right BA/Side Frame Long.	inch	Test Truck
7	Trail Left BA/Side Frame Long.	inch	Test Truck
8	Trail Right BA/Side Frame Long.	inch	Test Truck
9	Bolster/Body Vertical Displ.	inch	Test Truck
10	Train Speed	mph	Instr. Car
11	Automatic Location Device	volts	Test Truck
12	Average Truck Frame Distortion	mradians	Synthetic

4.2 WAYSIDE MEASUREMENTS

Data were recorded from two wayside instrumentation sites for all of the track tests. The test sections selected were located in the two-point contact profile section, at tie 1000 and in the buffer zone, preceding it at tie 895. Instrumentation was installed to measure vertical and lateral rail forces, lateral rail deflections and wheel set angles of attack. Table 3 lists the direct and synthetic wayside measurements.

Table 3. Wayside Measurement List

Measurement No.	Name	Units	Location
1	Inside Rail Vertical Force	kips	Tie #895
2	Inside Rail Lateral Force	kips	Tie #895
3	Outside Rail Vertical Force	kips	Tie #895
4	Outside Rail Lateral Force	kips	Tie #895
5	Inside Railhead Lat. Displ.	inches	Tie #895
6	Outside Railhead Lat. Displ.	inches	Tie #895
7	Wheel Set Angle of Attack	mradians	Tie #895
8	Inside Rail Vertical Force	kips	Tie #1000
9	Inside Rail Lateral Force	kips	Tie #1000
10	Outside Rail Vertical Force	kips	Tie #1000
11	Outside Rail Lateral Force	kips	Tie #1000
12	Inside Railhead Lat. Displ.	inches	Tie #1000
13	Outside Railhead Lat. Displ.	inches	Tie #1000
14	Wheel Set Angle of Attack	mradians	Tie #1000

4.3 WHEEL AND RAIL PROFILE MEASUREMENTS

A wheel profilometer was used to measure the wheel profiles from baseline car 310, bad actor cars 406, 366, 358, 334, 304, and AAR instrumented wheel sets 17 and 18. Rail profiles were measured with a rail profilometer at the wayside instrumentation sites located at ties 1000 and 895.

5.0 RESULTS

Results from the four track tests are presented in the order: (1) Baseline Car Test, (2) Bad Actor Car Test, (3) Truck Sequence Test, and (4) Tractive Effort Test. The major conclusion from the Baseline Car and Bad Actor Car tests was that neither car exhibited gage widening behavior when equipped with the instrumented wheel sets. Consequently, the Truck Sequence Test was modified to ensure that both test cars would be equipped with wheel sets that had previously been observed to produce gage widening. This had the desired effect of inducing the gage widening behavior in the two test cars. Thus, the behavior of the test cars in the Truck Sequence Test could be carefully compared to their behavior in the Baseline Car and Bad Actor Car tests.

Several comments on sign conventions are appropriate. First, the right hand rule sign convention was used for all of the test results presented in this report. That is, the direction of motion is positive, the orthogonal direction to the left is positive, and the vertical (up) direction is positive. Counterclockwise rotation about the vertical axis, when viewed from above, is positive. Also, the plots of truck frame warp angles include a double-headed arrow that designates the "warp" and "steer" directions defined for the truck distortion discussed in Section 3.1.2. It is important to distinguish the difference. Truck distortion in the "steer" direction is "normal" for a trailing three piece truck. It does not allow both wheel sets to develop large angles of attack or gage widening forces. Truck distortion in the "warp" direction, however, indicates that the truck frame was distorted such that both wheel sets will develop large angles of attack and potentially produce large gage widening forces.

5.1 BASELINE CAR ON DRY RAILS

5.1.1 Onboard Measurements

Figure 14 shows the truck moment plots for the baseline car tested on dry rails in the test curve. In the entry spiral, the turning moment between the truck and car body peaked at 230 kip-in and the steering moment was 30 kip-in. Both moments were applied to the truck in the CCW (positive) direction, which was the proper direction to rotate the truck through the curve. These moments were balanced by a clockwise (negative) warp moment of 260 kip-in created by lateral forces between the wheels and rails. The negative warp moment was in the "steer" direction and did not warp the truck frame.

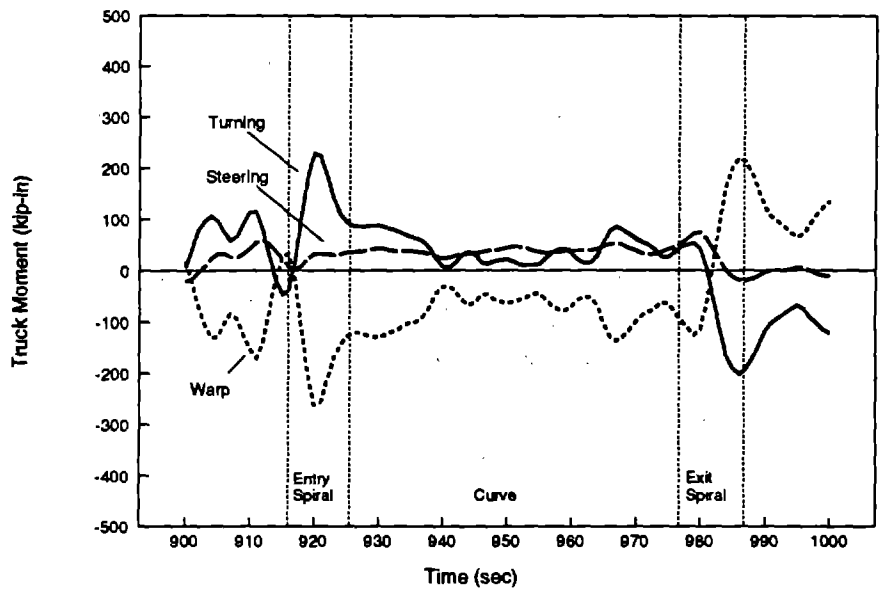

Figure 14. Baseline Car Truck Moments on Dry Rails

As expected, the turning moment between the car body and truck bolster peaked in the entry and exit spirals of the curve where the truck rotated relative to the car body. The truck bolster rotated -24 mradians relative to the car body in the entry spiral, as shown in Figure 15, which is approximately -3 mradians beyond radial alignment (-21 mradians relative rotation) in this curve, based on the car's truck spacing. The bolster rotated beyond radial alignment because the trailing wheel set maintained radial alignment in the curve, while the leading wheel set developed an angle of attack relative to the curve of approximately -6 mradians. The truck bolster, located mid-way between the wheel sets, developed an angle of attack equal to their average, or -3 mradians.

The truck frame deformation is also plotted in Figure 15 for the baseline car on dry rails. In the body of the curve, the truck frame distorted, that is, the truck bolster rotated relative to the side frames, approximately 10 mradians in the steer direction.

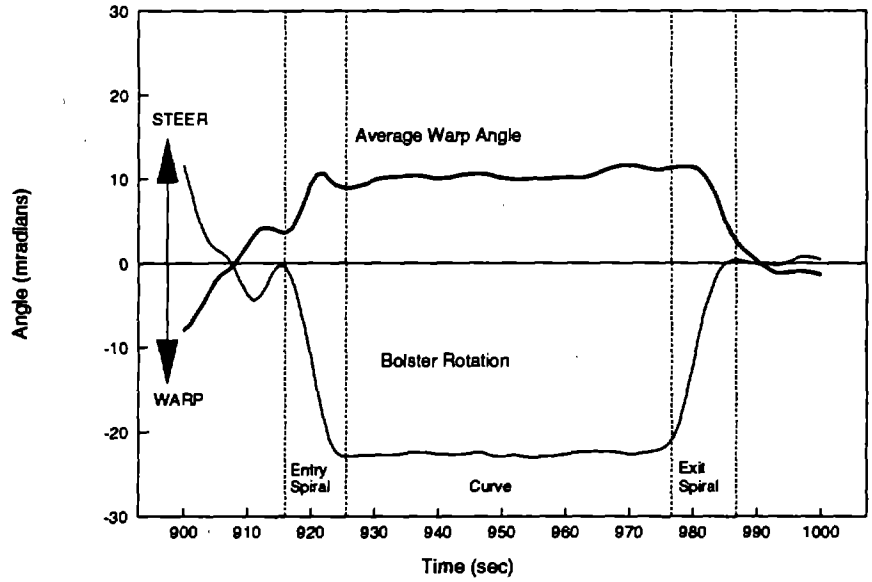

Figure 15. Baseline Car Truck Angles on Dry Rails

5.1.2 Wayside Measurements

Angles of attack of -6 and 0 mradians were measured for the leading and trailing wheel sets, respectively, of the test truck. The leading wheel set produced a low rail lateral force of 15 kips that deflected the low rail 0.1 inch. The trailing wheel set produced a lateral force of 3 kips and virtually no lateral rail deflection.

In this test, and all subsequent tests, the low rail lateral deflection was found to be much larger than the high rail, so only the low rail deflections are presented. This result supported the idea that larger overturning moments were applied to the low rail than the high rail because of the difference in points of contact, as described in Section 3.1.1.

5.2 BASELINE CAR ON LUBRICATED HIGH RAIL AND DRY LOW RAIL

5.2.1 Onboard Measurements

Figure 16 shows the truck moment plots for the baseline car tested on a lubricated high rail and dry low rail. In the entry spiral, the turning moment between the truck and car body peaked at 240 kip-in and the steering moment was 55 kip-in. Both moments were applied to the truck in the CCW (positive) direction, which was the proper direction to rotate the truck through the curve. These moments were balanced by a warp moment of -295 kip-in created by lateral forces between the wheels and rails. Again, the negative warp moment was in the steer direction and did not warp the truck frame.

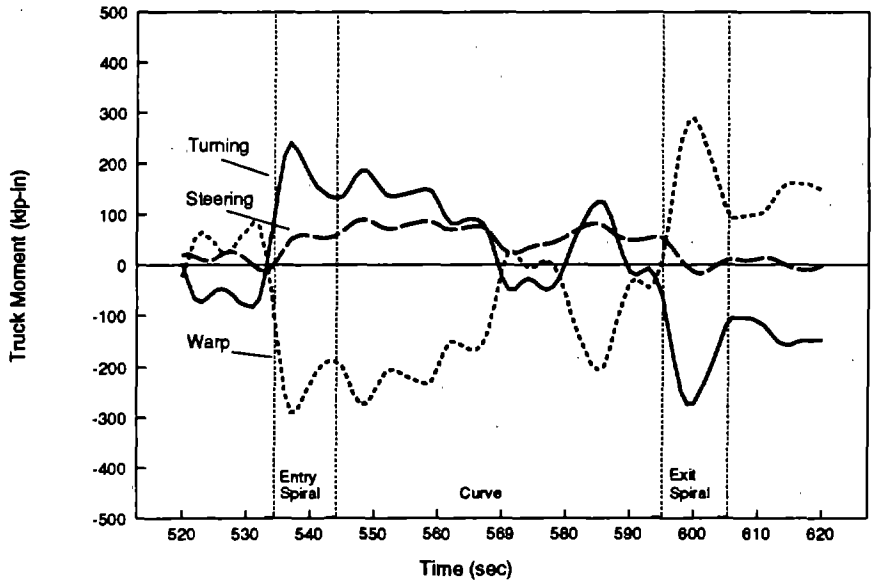

Figure 16. Baseline Car Truck Moments on Lubricated High Rail and Dry Low Rail

Through the curve, the truck steering moment increased until the car entered the Two-point Contact Grind Zone, at which point it decreased from almost 80 kip-inch to less than 40 kip-in. The direction of the warp moment reversed in this zone.

The bolster rotated -20 mradians (Figure 17) relative to the car body in the entry spiral, then rotated to -24 mradians in the Two-point Contact Grind Zone. The truck frame distorted by approximately 12 mradians in the steer direction.

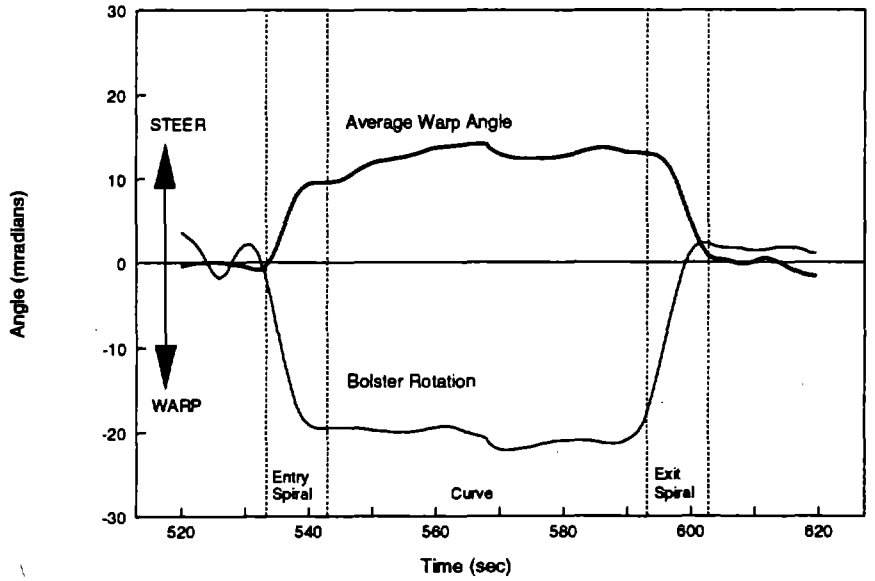

Figure 17. Baseline Car Truck Angles on Lubricated High Rail and Dry Low Rail

5.2.2 Wayside Measurements

The leading wheel set in the test truck developed an angle of attack of -7 mradians. This produced a lateral force of 9 kips that did not deflect the low rail. The trailing wheel set developed no angle of attack and produced a low rail lateral force of -1.0 kips that did not deflect the low rail.

5.3 BASELINE CAR ON LUBRICATED RAILS

5.3.1 Onboard Measurements

Figure 18 shows the truck moment plots for the baseline car tested on lubricated rails in the test curve. In the entry spiral, the turning moment between the truck and car body peaked at 180 kip-in and the steering moment was 60 kip-in. These moments were balanced by a warp moment of -240 kip-in created by lateral forces between the wheels and rails. Again, the negative warp moment was in the steer direction and did not warp the truck frame.

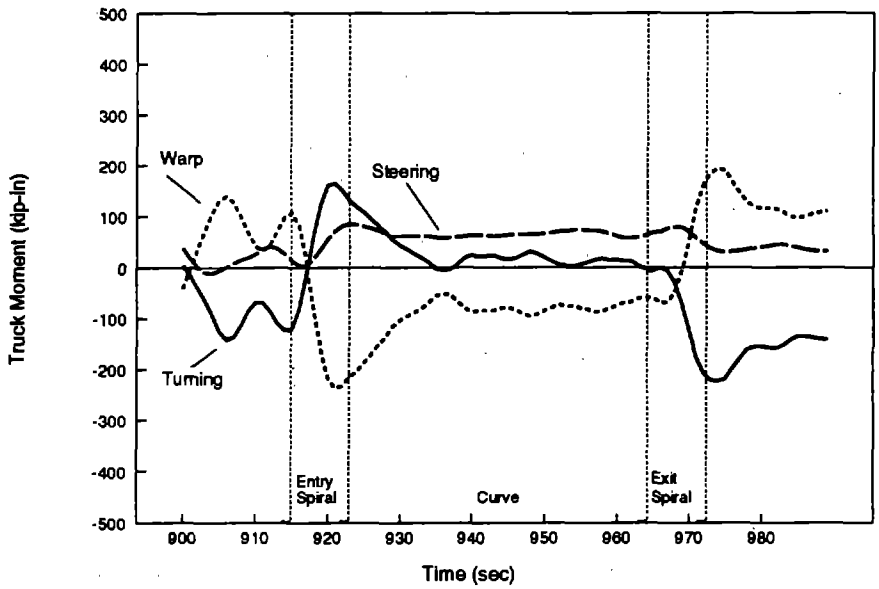

Figure 18. Baseline Car Truck Moments on Lubricated Rails

As shown in Figure 19, the bolster rotated -19 mradians relative to the car body in the entry spiral. The truck frame distorted approximately 5 mradians in the steer direction.

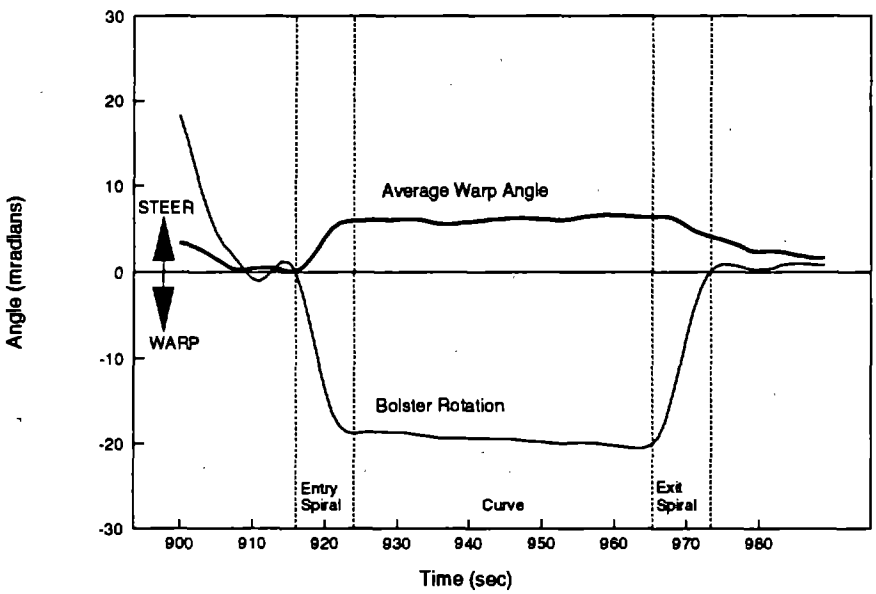

Figure 19. Baseline Car Truck Angles on Lubricated Rails

5.3.2 Wayside Measurements

The leading wheel set in the test truck had an angle of attack of -7 mradians. This produced a lateral force of 7 kips that did not deflect the low rail. The trailing wheel set developed no angle of attack and produced a low rail lateral force of 1 kip that did not deflect the low rail.

5.4 BAD ACTOR CAR ON DRY RAILS

5.4.1 Onboard Measurements

Figure 20 shows the truck moment plots for the bad actor car tested on dry rails in the test curve. In the entry spiral, the turning moment between the truck and car body peaked at 100 kip-in, and the steering moment was 40 kip-in. These moments were balanced by a warp moment of -140 kip-in, created by lateral forces between the wheels and rails. As in the Baseline Car Test, the negative warp moment was in the steer direction and did not warp the truck frame.

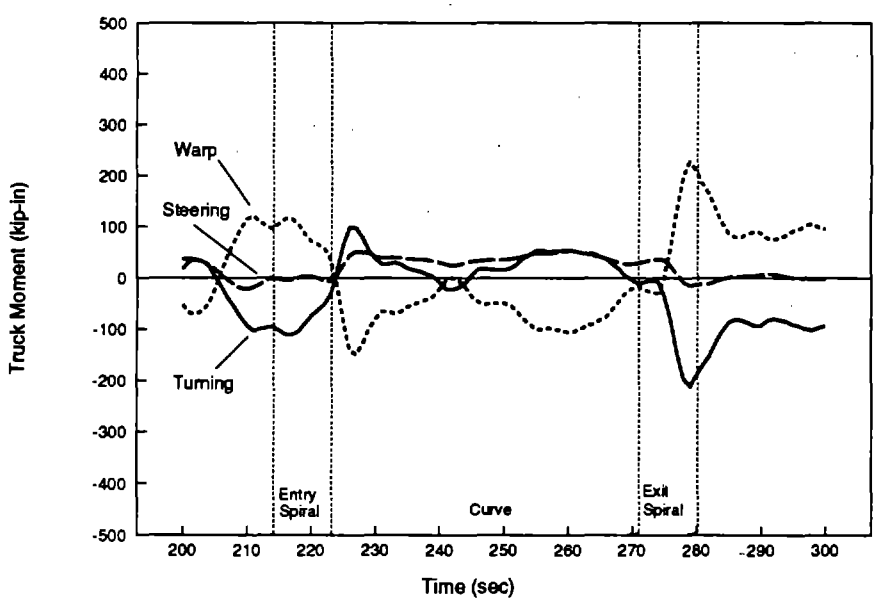

Figure 20. Bad Actor Car Truck Moments on Dry Rails

As shown in Figure 21, the bolster rotated -24 mradians relative to the car body in the entry spiral, which is approximately -3 mradians beyond radial alignment in this curve. The truck frame distorted approximately 7 mradians in the steer direction.

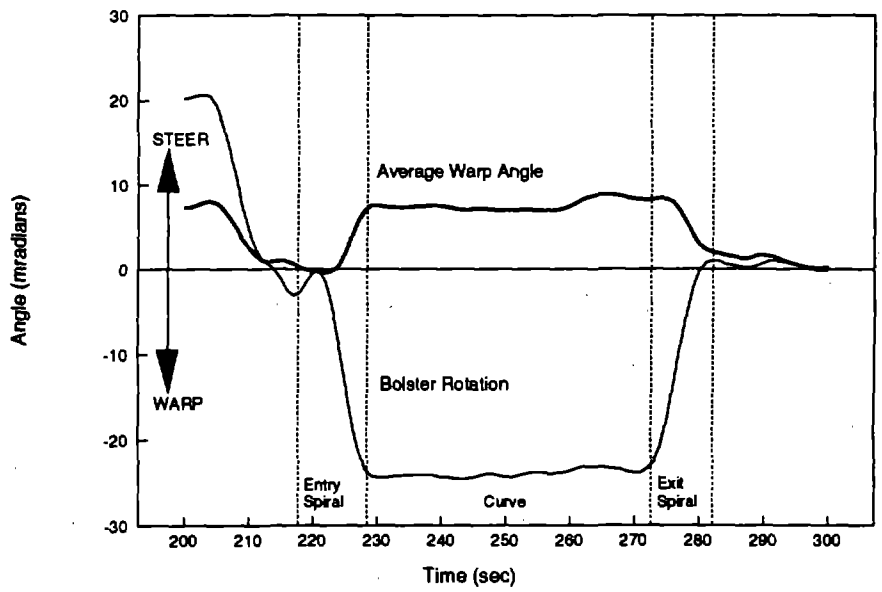

Figure 21. Bad Actor Car Truck Angles on Dry Rails

5.4.2 Wayside Measurements

The leading wheel set in the test truck had an angle of attack of -6 mradians. This produced a lateral force of 10 kips that, in turn, deflected the low rail 0.1 inch. The trailing wheel set developed no angle of attack and produced a low rail lateral force of 2 kips that did not deflect the low rail.

5.5 BAD ACTOR CAR ON LUBRICATED HIGH RAIL AND DRY LOW RAIL

5.5.1 Onboard Measurements

Figure 22 shows the truck moment plots for the bad actor car tested on a lubricated high rail and dry low rail. In the entry spiral, the turning moment between the truck and car body peaked at 140 kip-in, and the steering moment was 50 kip-in. These moments were balanced by a warp moment of -190 kip-in, created by lateral forces between the wheels and rails. Again, the negative warp moment was in the steer direction and did not warp the truck frame.

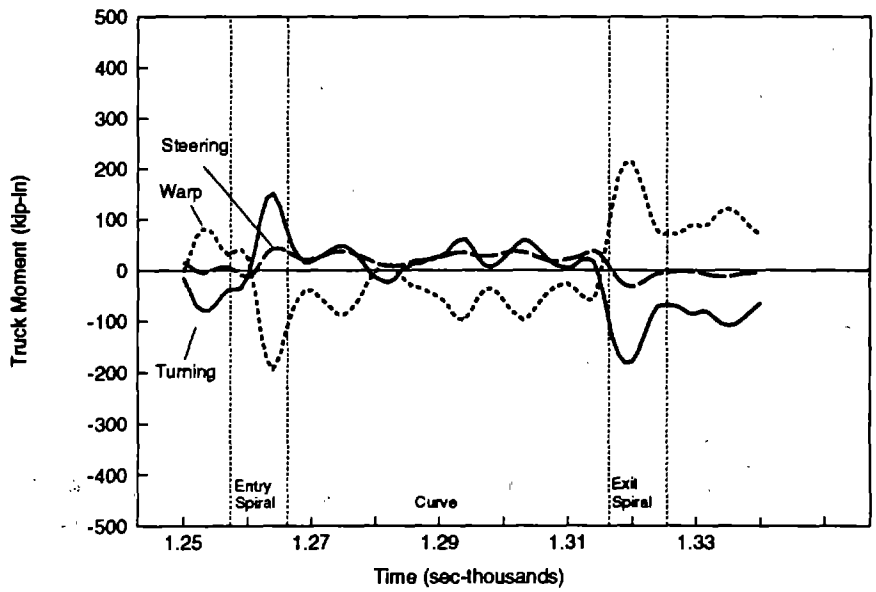

Figure 22. Bad Actor Car Truck Moments on Lubricated High Rail and Dry Low Rail

As shown in Figure 23, the bolster rotated -24 mradians relative to the car body in the entry spiral, which is approximately -3 mradians beyond radial alignment in this curve. The truck frame distorted approximately 9 mradians in the steer direction.

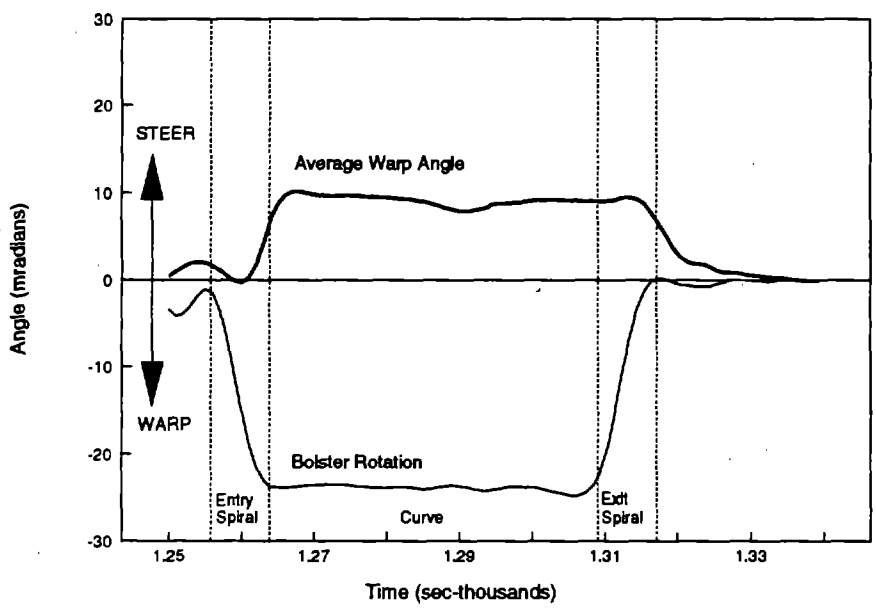

Figure 23. Bad Actor Car Truck Angles on Lubricated High Rail and Dry Low Rail

5.5.2 Wayside Measurements

The leading wheel set in the test truck had an angle of attack of -4 mradians. This produced a low rail lateral force of 12 kips that deflected the low rail 0.1 inch. The trailing wheel set developed no angle of attack and produced a low rail lateral force of 2 kips that did not deflect the low rail.

5.6 BAD ACTOR CAR ON LUBRICATED RAILS

5.6.1 Onboard Measurements

Figure 24 shows the truck moment plots for the bad actor car tested on lubricated rails in the test curve. In the entry spiral, the turning moment between the truck and car body peaked at 120 kip-in, and the steering moment was 50 kip-in. These moments were balanced by a warp moment of -170 kip-in, created by lateral forces between the wheels and rails. Again, the negative warp moment was in the steer direction and did not warp the truck frame.

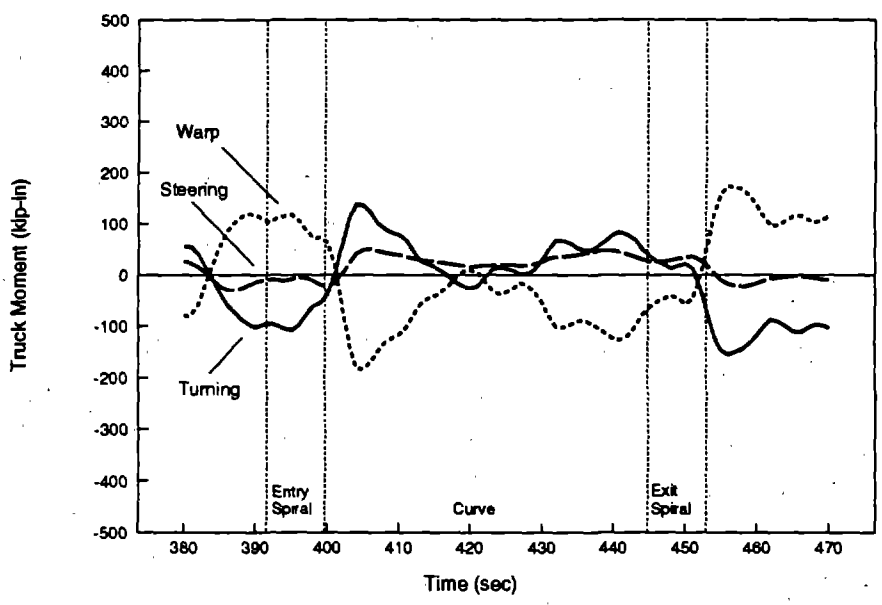

Figure 24. Bad Actor Car Truck Moments on Lubricated Rails

As shown in Figure 25, the bolster rotated -24 mradians relative to the car body in the entry spiral, which is approximately -3 mradians beyond radial alignment in this curve. The truck frame distorted approximately 4 mradians in the steer direction.

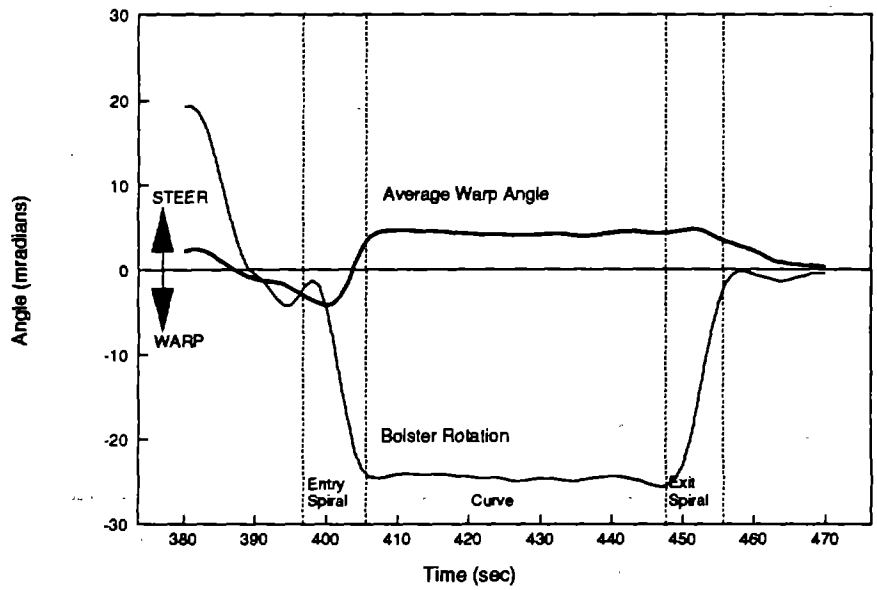

Figure 25. Bad Actor Car Truck Angles on Lubricated Rails

5.6.2 Wayside Measurements

The leading wheel set in the test truck had an angle of attack of -6 mradians. This produced a lateral force of 8 kips that did not deflect the low rail. The trailing wheel set developed no angle of attack and produced a low rail lateral force of 2 kips that did not deflect the low rail.

5.7 TRUCK SEQUENCE TEST

For this test, wheel sets from car 366, a former bad actor, were installed in the baseline car (310). The bad actor car (406) was equipped with its original wheel sets. The first test series was conducted after the FAST-HAL train made several laps through the test zone to dry the track. Both railheads were very dry (u>0.5), but the gage face of the high rail remained lubricated.

Figure 26 shows low rail lateral forces and deflections measured when the bad actor cars and test cars passed over the Two-point Contact Grind Zone instrumented rails. Some of the bad actor trucks produced lateral forces exceeding 25 kips and low rail displacements approaching 0.5 inch. When the lubrication level increased until the head of the high rail became lubricated, however, the gage widening diminished, as shown in Figure 27.

The largest gage widening displacements were produced by the sequence of four trucks, beginning with the trailing truck of car 304 and ending with the leading truck of car 334. Note that both trucks of the middle car (358) were spreading the gage. Comparing the gage widening produced by this sequence of trucks to that produced by the trailing truck of car 375 and the leading truck of car 319 clearly demonstrates the rail restraining effect of an adjacent non-gage widening truck.

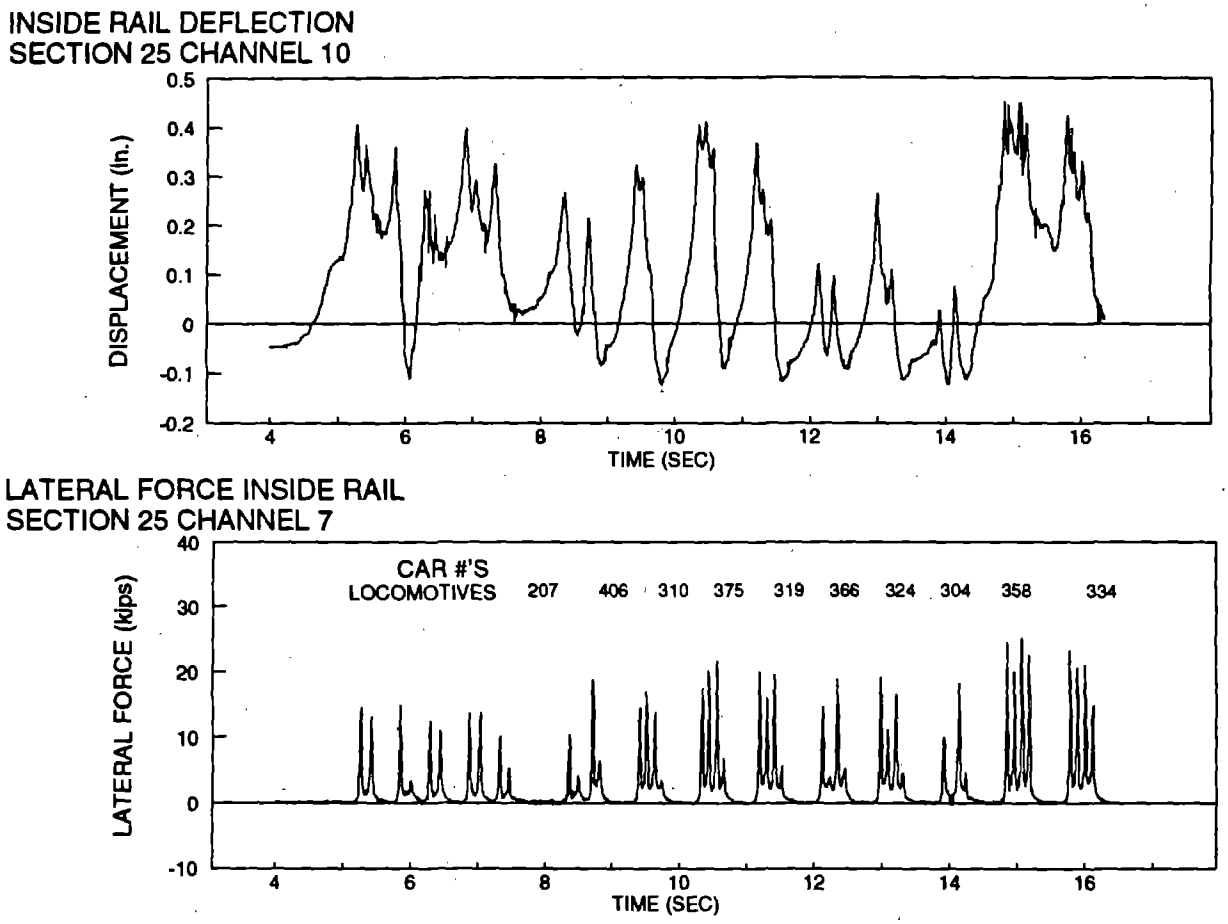

Figure 26. Inside Rail Lateral Deflections and Forces with Lubricated Gage Face

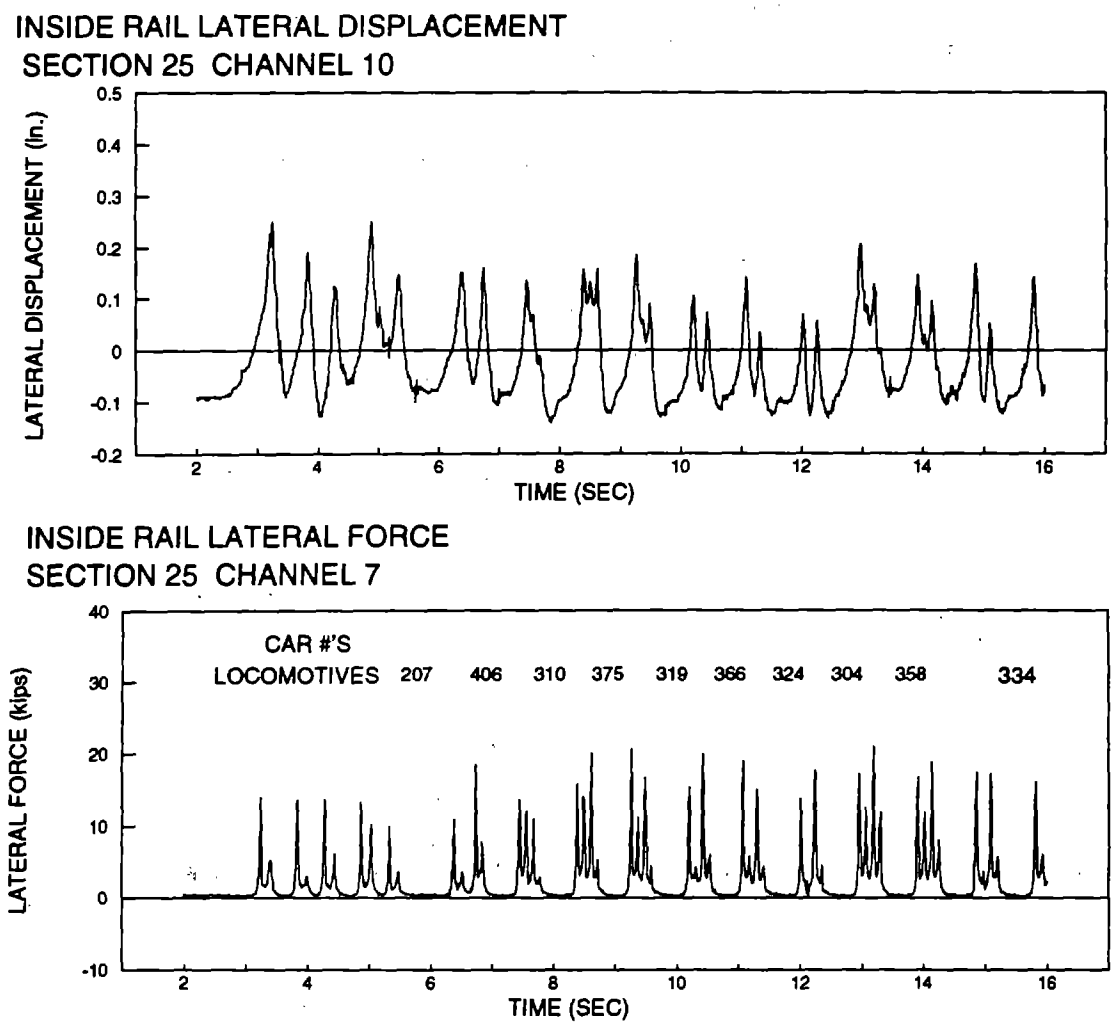

Figure 27. Inside Rail Lateral Deflections and Forces with Lubricated High Rail

In contrast to the earlier tests with instrumented wheel sets, the trailing trucks of both the bad actor car and the baseline car produced excessive gage widening when equipped with wheel sets from previous bad actors. The leading wheel set in the trailing truck of car 406 developed an angle of attack of 6 mradians and a low rail lateral force of 15 kips. The trailing wheel set developed an angle of attack of 4 mradians and a low rail lateral force of 19 kips. Together, the low rail wheels produced a low rail truck-side L/V ratio of 0.55 and a low rail lateral deflection of 0.33 inch. The leading wheel set in the trailing truck of car 310 developed an angle of attack of 8 mradians and a low rail lateral

force of 19 kips. The trailing wheel set developed an angle of attack of 5 mradians and a low rail lateral force of 22 kips. Together, the low rail wheels produced a low rail truck-side L/V ratio of 0.6 and a low rail lateral deflection of 0.40 inch.

The net truck warp moments were calculated from the wayside lateral forces for the trailing trucks of both test cars. The warp moments were found to have reversed in direction from the previous tests, measuring +100 and +290 kip-in in the *warp* direction, respectively, for the baseline and bad actor cars. These results indicated that the net truck steering moments had reversed to the negative, or "anti-steering", direction. To derive the truck steering moments, the trailing truck turning moments previously measured for the baseline car (approximately +250 kip-in) and the bad actor car (approximately +100 kip-in) were added to their measured warp moments. The results were "anti-steering" moments of -350 kip-in for the baseline car and -390 kip-in for the bad actor car.

As shown in Figure 28, the trailing truck bolster of car 406 rotated -29 mradians relative to the car body in the two point contact grind zone, which is approximately -8 mradians beyond radial alignment (-21 mradians relative rotation) in this curve. The bolster rotated well beyond radial alignment because the truck frame warped and both wheel sets developed a negative angle of attack. A -8 mradians bolster rotation beyond radial alignment indicates that the trailing wheel set developed an angle of attack of approximately 5 mradians. The truck frame distorted by 12 mradians in the warp direction, indicating that the truck frame had indeed warped.

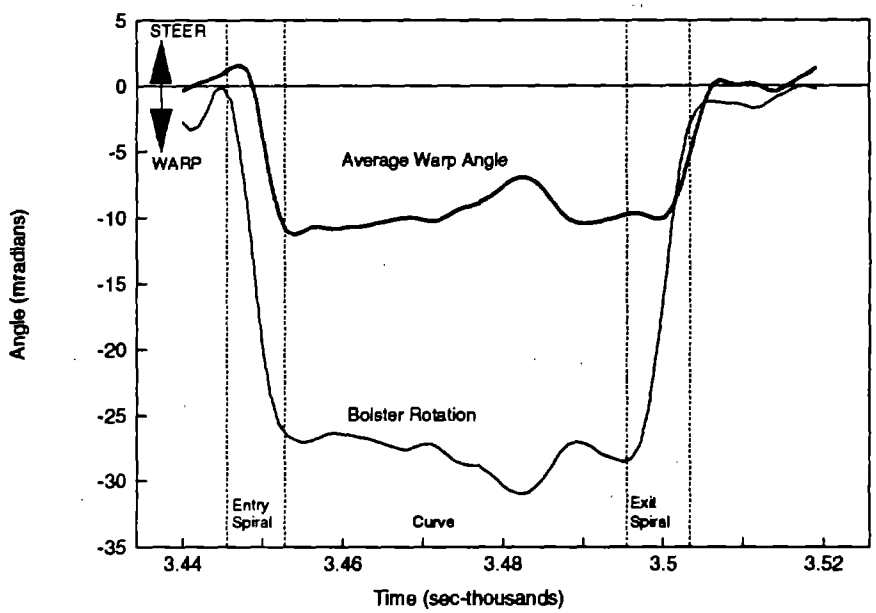

Figure 28. Car 406 Truck Angles

5.8 WHEEL AND RAIL PROFILE MEASUREMENTS

Wheel profiles measurements were taken from AAR instrumented wheel sets 17 and 18, baseline car 310, and bad actor cars 406, 366, 358, 334, and 304. In general, wheels of the bad actors were found to have practically no conicity or taper across the tread when compared to the instrumented wheel sets and the wheel sets of baseline car 310. Rail profile measurements were taken at the two wayside instrumentation locations; in the Two-point Contact Grind Zone and in the preceding buffer zone.

When overlaid, the instrumented wheel sets and baseline car 310 wheel sets appeared to conform much more closely to the Two-point Contact Grind Zone rail than the wheels of the bad actor cars (see Figure 29). This supported the idea that two-point contact between the wheel and rail caused, under certain lubrication conditions, a reversal of the steering moment as described in Section 3.1.4.

Figure 29. Instrumented Wheel Set and Car 406 Wheel Profiles

5.9 MODEL WITH INSTRUMENTED WHEEL SET PROFILES

Figure 30 shows the trailing truck turning moments predicted by the HAL car simulation using instrumented wheel set No. 17 wheel profiles and operated in a 6-degree curve with the low and high railheads dry (u=0.6) and the high rail gage face lubricated (u=0.1). A friction moment of 100 kip-in between the car body and truck bolster was used to represent the 100 kip-inch turning moment measured for the bad actor car. The steering and warp moments were approximately 25 and -20 kip-in, respectively, in the body of the curve. The negative warp moment reaction was in the steer direction and did not warp the truck frame.

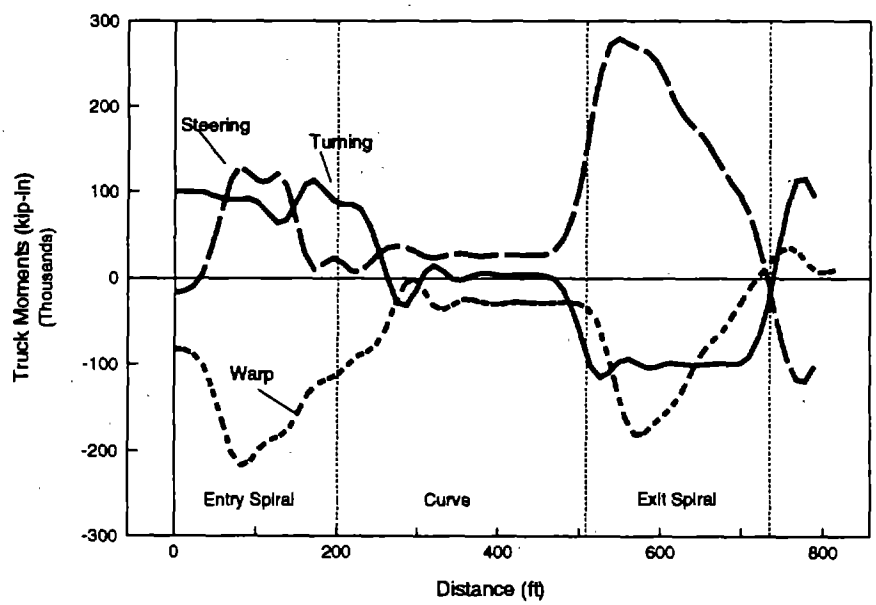

Figure 30. Instrumented Wheel Set Model Truck Moments on Lubricated Gage Face

Figure 31 shows the truck bolster rotation and truck frame distortion angles predicted by the NUCARS model. The truck bolster rotated -19 mradians relative to the car body, and the truck frame distorted approximately 6 mradians in the steer direction.

The NUCARS model predicted that the leading wheel set would develop an angle of attack of 6 mradians and the trailing wheel set would remain in radial alignment with the curve. As a result, only the leading wheel set developed large lateral forces. The trailing wheel set developed virtually no lateral force, and the truck-side L/V ratio, which is used to assess rail rollover potential, remained low.

These results are consistent with the results of the Baseline Car and Bad Actor Car tests, where the instrumented wheel sets were used.

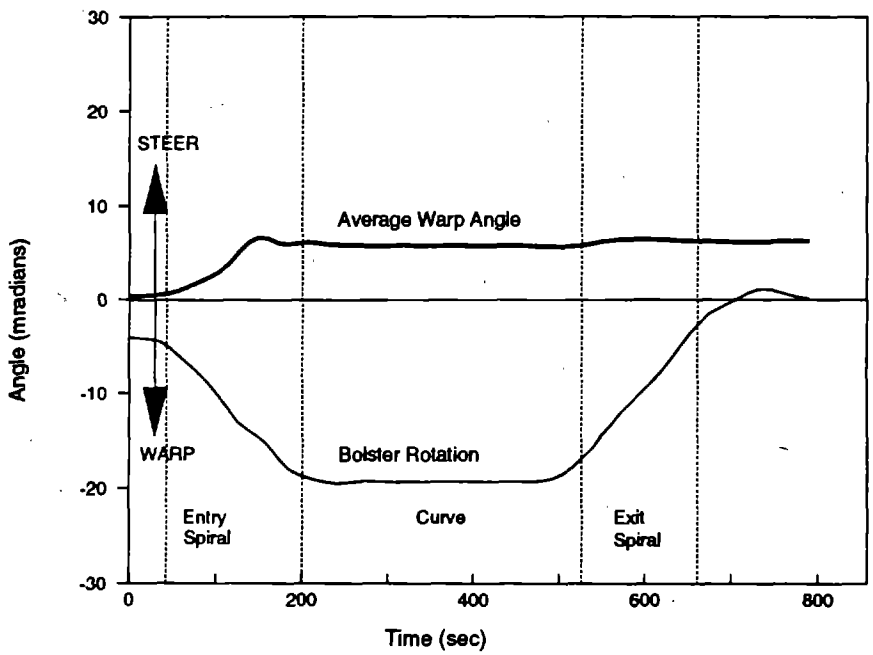

Figure 31. Instrumented Wheel Set Model Truck Angles on Lubricated Gage Face

5.10 MODEL WITH CAR 406 WHEEL PROFILES

Figure 32 shows the truck turning moments predicted by the HAL car simulation using car 406 wheel set No. 4 wheel profiles and operated in a curve with the low and high railheads dry (u=0.6) and the high rail gage face lubricated (u=0.1). The steering moment of -200 kip-in is now reversed from that predicted by the instrumented wheel set model. It is applied to the truck in the direction opposing proper rotation in the curve. This

"anti-steering" moment was balanced by the turning moment of approximately 40 kip-in and the warp moment of approximately 160 kip-in. The positive warp moment reaction was in the warp direction and acted to warp the truck frame.

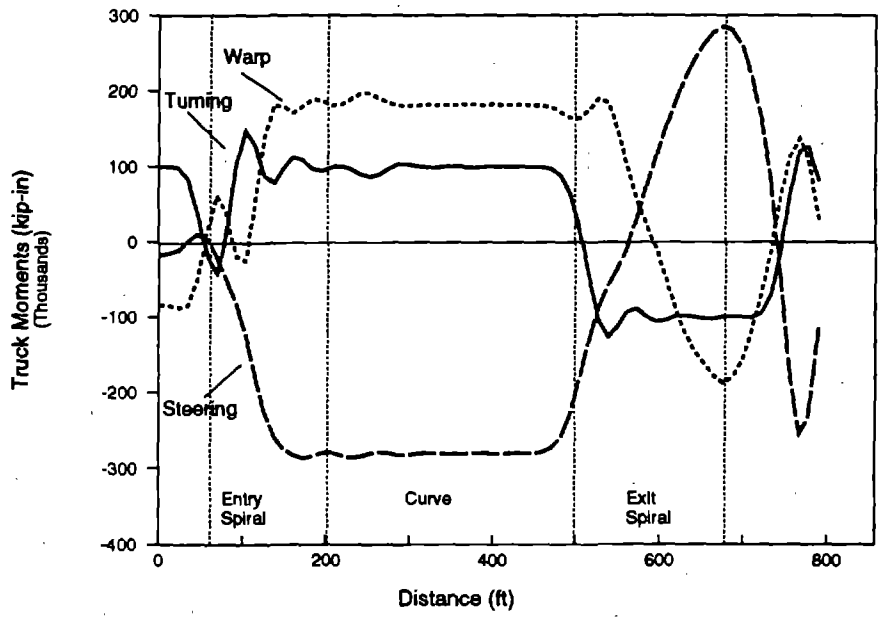

Figure 32. Car 406 Model Truck Moments on Lubricated Gage Face

Figure 33 shows the truck bolster rotation and truck frame warp angles predicted by the NUCARS model. The truck bolster rotated -23 mradians relative to the car body, and the truck frame distorted -6 mradians in the *warp* direction. These indicate that the 160 kip-in warp moment was sufficient to warp the model truck frame such that both wheel sets developed significant angles of attack.

The leading wheel set developed an angle of attack exceeding 9 mradians, and the trailing wheel set developed an angle of attack of 3 mradians. As a result, the predicted truck-side L/V ratio reached 0.5, approaching the AAR *Manual of Standards and Recommended Practices*, Chapter XI maximum limit for this criterion of 0.6.

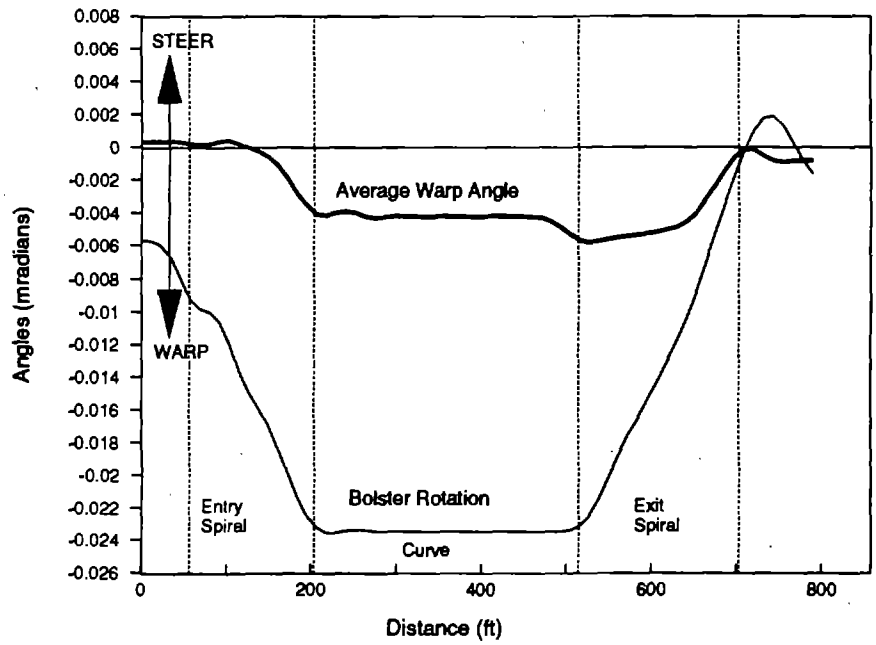

Figure 33. Car 406 Model Truck Angles on Lubricated Gage Face

These predictions are consistent with the results of the Truck Sequence Test, where the bad actor car 406 was equipped with its original wheel sets. In both cases, the truck warped and both wheel sets developed large angles of attack. The modeling study further demonstrated that the very low taper or conicity wheel profiles of car 406 developed a negative longitudinal creep force on the tread and a positive longitudinal creep force on the flange. On dry rails, the positive flange longitudinal creep force exceeds the negative tread longitudinal creep force and, thus, the net longitudinal wheel force is positive. But when the gage face of the high rail is lubricated, and the top of the rail remains dry, the positive flange longitudinal creep force is drastically reduced. As a result, the negative tread longitudinal creep force exceeds that of the flange and the net leading wheel set steering moment becomes negative. Combining this with the negative trailing wheel set steering moment produces a large net negative steering moment that exceeds the positive turning moment. The magnitude by which it exceeds the turning moment is larger than the truck's warp restraint, thereby warping the truck.

5.11 TRACTIVE EFFORT TEST

Figure 34 shows the lateral forces and rail deflections produced by the locomotives passing over the Two-point Contact Grind Zone when both rails were dry. In Figure 35, the low rail was dry and the high rail was lubricated. The trailing wheel set lateral forces increased dramatically during the second test, producing a maximum truck-side L/V ratio exceeding 0.5. The resulting rail deflections approached 0.4 inch on the low rail.

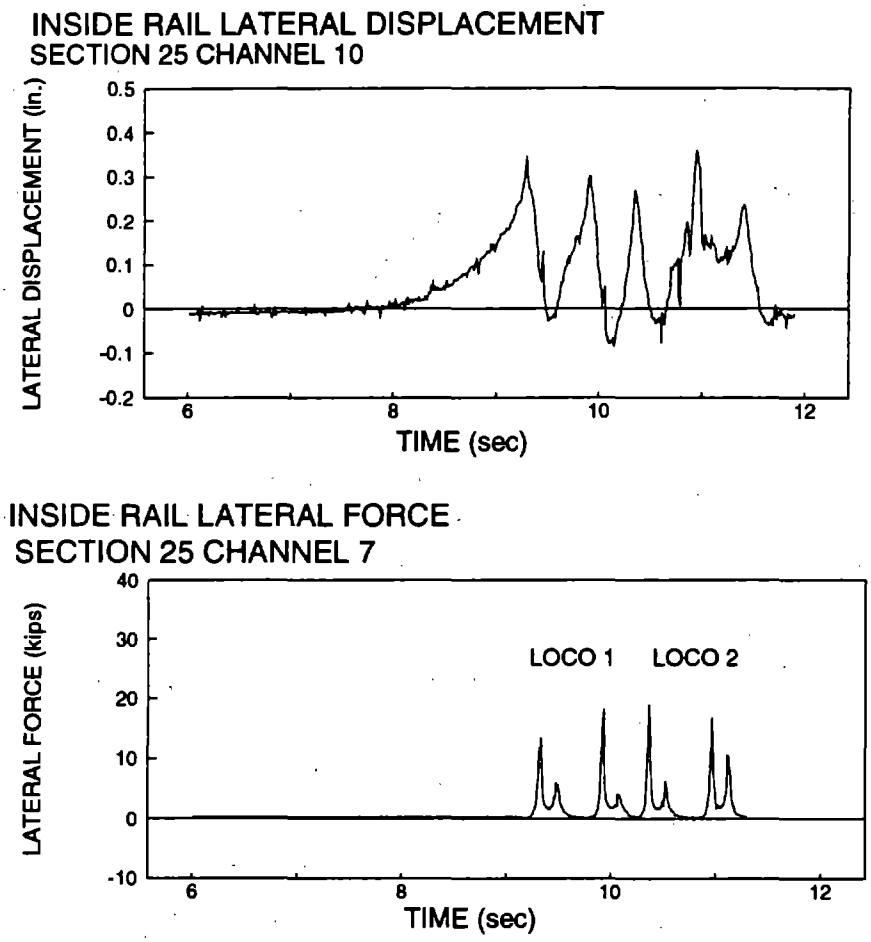

Figure 34. Inside Rail Lateral Deflections and Forces with Dry Rail

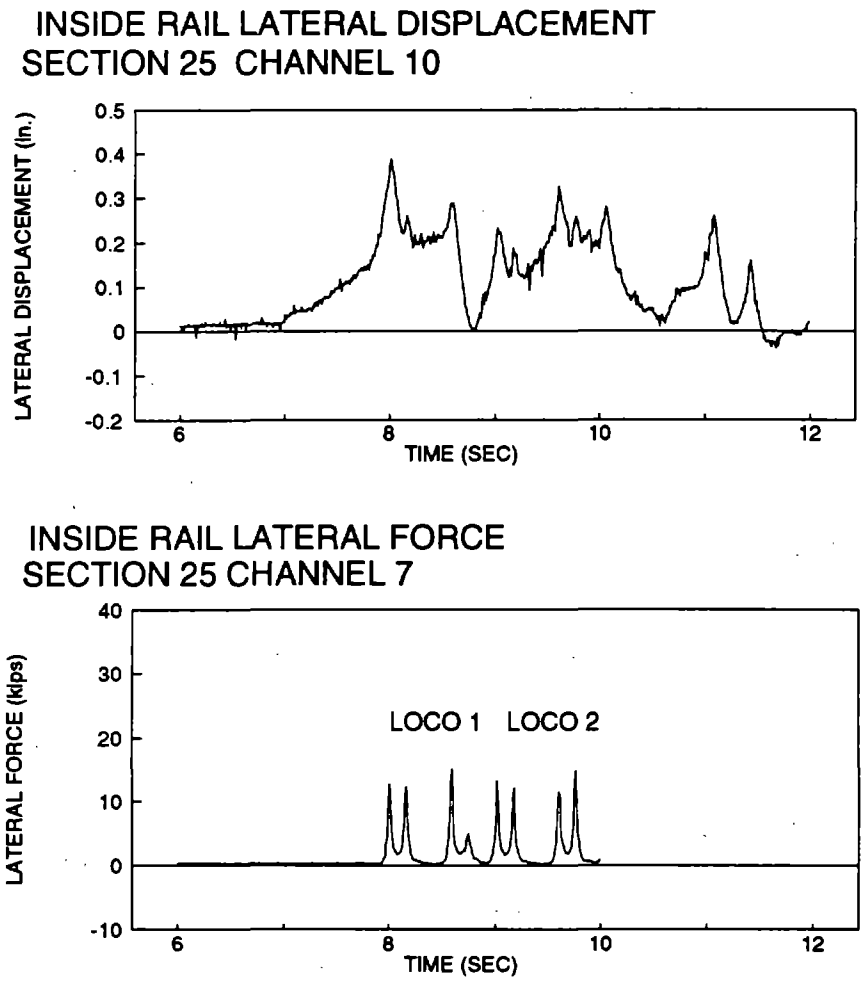

Figure 35. Inside Rail Lateral Deflections and Forces with Lubricated High Rail

Figure 36 illustrates how, under conditions of differential rail lubrication, a large truck moment can be developed that causes the wheel sets to produce large gage widening forces. When the low rail is dry and the high rail is well lubricated, the tractive or longitudinal force developed by the wheel on the low rail is much larger than that developed on the high rail. As a result of this imbalance in longitudinal forces, a large moment is applied to the truck in the direction shown. This moment is reacted by lateral wheel forces that are produced when all of the wheel sets in the truck develop angles of attack. As a consequence of this, large gage widening forces are produced.

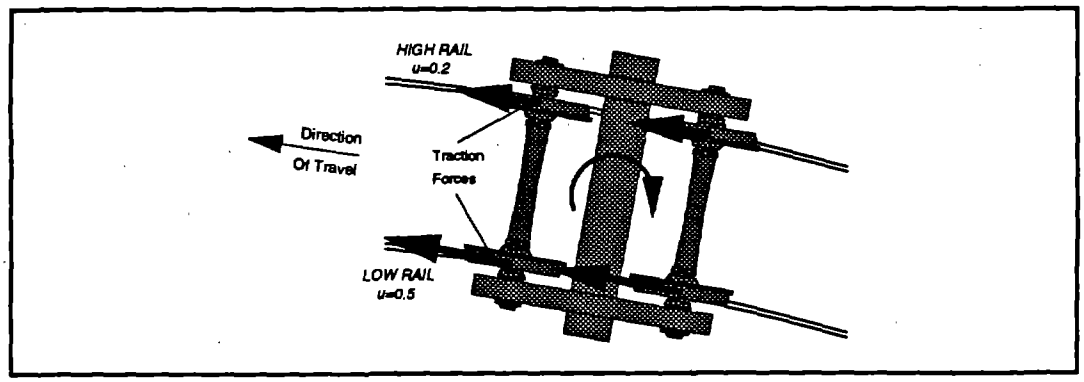

Figure 36. Locomotive Truck Turning Moment

6.0 DISCUSSION OF RESULTS

During the Truck Sequence Test, gage widening forces were produced by both test cars and many of the bad actor cars. Measurements indicated that the gage widening trucks had warped, which allowed both of their wheel sets to develop large angles of attack and lateral forces. The trucks warped when excessive positive warp moments were generated by the wheel sets in reaction to a net negative truck steering moment. The net truck steering moment was negative because both wheel sets produced negative steering moments. This is in contrast to the previous tests, with instrumented wheel sets, in which the leading wheel set produced a positive steering moment that exceeded the negative steering moment of the trailing wheel set. Three combining factors caused the leading wheel sets of the bad actor cars to produce negative steering moments: (1) two-point contact occurred between the high rail and wheel, (2) the bad actor wheels had low conicity or taper across the wheel treads, and (3) the coefficient of friction between the high rail and wheel flange was reduced by lubrication.

The high rail wheel of the leading wheel sets in each truck contacted the rail in the two-point grind zone at two points, one point on the flange and the other on the tread. Longitudinal creep forces were produced by both the tread and flange contact points of the high rail wheel. The direction and magnitude of these creep forces varied, depending on the contact between the rail and wheels.

Examination of the wheel profiles in conjunction with the model predictions indicated that the instrumented wheel sets produced a positive longitudinal creep force on both contact points of the high rail wheel. This was due to the high conicity, or taper of the instrumented wheel sets that caused both contact points of the high rail wheel to have

a significantly larger rolling radius than the contact point of the low rail wheel. The bad actor wheel sets, however, had very low conicity. As a result, the high rail wheel tread contact point was located on a rolling radius similar to that of the low rail wheel. This caused a negative longitudinal creep force to be produced by the tread contact point of the high rail wheel.

When the high rail was dry or uniformly lubricated; i.e., the gage face coefficient of friction was approximately the same as that of the railhead, the longitudinal creep force developed by the high rail wheel flange exceeded that of the tread, and the wheel set net steering moment was positive. But when the gage face of the high rail was lubricated and the head remained dry, the tread longitudinal creep force exceeded that of the flange. With the instrumented wheel sets, a positive net longitudinal high rail wheel force was still produced because the tread produced a positive longitudinal creep force. With the bad actor wheel sets, however, a negative net longitudinal wheel force was produced because the deficient tread taper produced a negative longitudinal creep force. This caused the steering moment of the leading wheel set to become negative.

This explains why the test trucks exhibited gage widening behavior only when equipped with bad actor (low conicity) wheel sets and only when the gage face of the high rail was well lubricated, and the railheads were dry.

7.0 CONCLUSIONS

1. In both the Baseline and Bad Actor Car Tests, the test truck with instrumented wheel sets exhibited "typical" behavior for a trailing truck during curve negotiation; that is, the leading wheel set developed an angle of attack while the trailing wheel set remained radially aligned with the curve.

2. In both the Baseline and Bad Actor Car Tests, the test trucks exhibited truck moments that were typical of a trailing truck during curve negotiation. The turning and steering moments were applied in the proper direction to turn the truck through the curve and were balanced by a warp moment in the opposite direction.

3. In both the Baseline and Bad Actor Car Tests, varying the track lubrication did not cause the test cars to exhibit gage widening behavior.

4. In the Truck Sequence Test, replacing the instrumented wheel sets in the test cars with bad actor wheel sets appeared to instigate gage widening behavior when the gage face of the high rail was lubricated and the railheads were dry. Several bad actor cars also exhibited gage widening behavior.

5. In the Truck Sequence Test, the gage widening trucks warped when their steering moments reversed from the desired positive direction and caused a large positive warp moment to be produced.

6. In the Truck Sequence Test, where several gage widening trucks were adjacent in the consist, large sustained gage widening was produced with displacements exceeding 0.5 inch.

7. In the Truck Sequence Test, when lubricant migrated to the head of the high rail, the gage widening diminished because the net truck steering moments were once again in the positive direction.

8. The NUCARS-HAL car model predictions demonstrated that the steering moment in the truck could be reversed if the high rail contacted the wheel flange and tread simultaneously. The high rail tread contact point produced a negative longitudinal creep force due to low conicity, and the tread longitudinal creep force exceeded that of the flange due to gage face lubrication.

9. The current practice at FAST of providing some lubrication to both the high and low rail should prevent the generation of large lateral creep forces on the low rail, as long as the lubricant is applied to the head of the low rail.

10. The gage widening behavior observed at FAST could occur in revenue service, since two-point contact, low conicity wheels and high rail gage face lubrication are often encountered. It is common practice, in fact, to grind off the gage corner of the high rail in curves, forcing two-point contact, and lubricate only the high rail gage face.

11. In all tests, the low rail lateral deflections were much larger than the high rail because larger overturning moments were applied to the low rail than to the high rail. The difference in low and high rail overturning moments

was due to the different points of contact between the wheels and rails. In general, much large overturning moments will be applied to the low rail than the high rail in a curve by a flanging wheel set.

12. Under conditions of differential lubrication, the tractive effort forces generated by the locomotives produced truck turning moments that were reacted by large lateral forces at the rails. As a result, gage widening displacements exceeding 0.5 inch were produced. The magnitude of the lateral gage widening forces was proportional to the tractive effort of the locomotives.

8.0 RECOMMENDATIONS

1. Severe two-point contact between the wheels of the HAL cars and the rails should be avoided by maintaining conformal or single-point contact wheel and rail profiles.

2. The combination of a dry low rail and a high rail with lubricated gage face and dry head in curves should be avoided by ensuring the high railhead is well lubricated and the low railhead is lightly lubricated.

3. In curves where gage corner grinding is practiced, the lateral track strength should be increased by installing elastic fasteners, rather than cut spikes.

4. Some means of increasing the warp restraint of three-piece trucks, such as frame bracing, should be used to reduce the incidences of truck frame warping and production of large gage widening forces.

References

1. Elkins, J.A. Weinstock, H. "The Effect of Two Point Contact on the Curving Performance of Railroad Vehicle," ASME Paper No. 82-WQ/DSC-13, November 1982.

DISCLAIMER

This document is disseminated under the sponsorship of the Department of Transportation in the interest of information exchange. The United States Government assumes no liability for the contents or use thereof. The United States Government does not endorse products or manufacturers. Trade or manufacturers' names appear herein solely because they are considered essential to the object of this report.